LBNL-41950

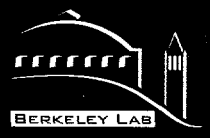

ERNEST ORLANDO LAWRENCE
BERKELEY NATIONAL LABORATORY

Exploratory Technology Research Program for Electrochemical Energy Storage

Annual Report for 1997

Kim Kinoshita, Editor

Environmental Energy Technologies Division

June 1998

DISCLAIMER

Portions of this document may be illegible in electronic image products. Images are produced from the best available original document.

LBNL-41950

EXPLORATORY TECHNOLOGY RESEARCH PROGRAM FOR ELECTROCHEMICAL ENERGY STORAGE

ANNUAL REPORT FOR 1997

Environmental Energy Technologies Division
Lawrence Berkeley National Laboratory
University of California
Berkeley, California 94720

Edited by Kim Kinoshita, Technical Manager

June 1998

This work was supported by the Assistant Secretary for Energy Efficiency and Renewable Energy, Office of Transportation Technologies, Office of Advanced Automotive Technologies of the U.S. Department of Energy under Contract No. DE-AC03-76SF00098.

CONTENTS

COMPONENTS FOR NONAQUEOUS CELLS

CROSS-CUTTING RESEARCH

PROGRAM SUMMARY

The U.S. Department of Energy's (DOE) Office of Transportation Technologies provides support for an Electrochemical Energy Storage Program, that includes research and development on advanced rechargeable batteries. A major goal of this program is to develop electrochemical power sources suitable for application in electric vehicles (EVs) and hybrid systems. The program centers on advanced electrochemical systems that offer the potential for high performance and low life-cycle costs, both of which are necessary to permit significant penetration into commercial markets.

The DOE Electric Vehicle Technology Program is divided into two project areas: the United States Advanced Battery Consortium (USABC) and Advanced Battery R&D which includes the Exploratory Technology Research (ETR) Program managed by the Lawrence Berkeley National Laboratory* (LBNL). The USABC, a tripartite undertaking between DOE, the U.S. automobile manufacturers and the Electric Power Research Institute (EPRI), was formed in 1991 to accelerate the development of advanced batteries for EVs. In addition, DOE is actively involved in the Partnership for a New Generation of Vehicles Program (PNGV) which seeks to develop passenger vehicles with a fuel economy equivalent to 80 mpg of gasoline. The role of the ETR Program is to perform supporting research on the advanced battery systems under development by the USABC and PNGV Programs, and to evaluate new systems with potentially superior performance, durability and/or cost characteristics. The specific goal of the ETR Program is to identify the most promising electrochemical technologies and transfer them to the USABC, the battery industry and/or other Government agencies for further development and scale-up. This report summarizes the research, financial and management activities relevant to the ETR Program in CY 1997. This is a continuing program, and reports for prior years have been published; they are listed at the end of this Executive Summary.

The general R&D areas addressed by the program include identification of new electrochemical couples for advanced batteries, determination of technical feasibility of the new couples, improvements in battery components and materials, and establishment of engineering principles applicable to electrochemical energy storage. Major emphasis is given to applied research which will lead to superior performance and lower life-cycle costs.

---

* Participants in the ETR Program include the following LBNL scientists: E. Cairns, J. Evans, J. Kerr, K. Kinoshita, F. McLarnon and J. Newman of the Environmental Energy Technologies Division; and L. De Jonghe and P. Ross and of the Materials Sciences Division.

RESEARCH PROJECT HIGHLIGHTS

The ETR Program focuses on research that provides and establishes scientific and engineering principles applicable to batteries; and to identify, characterize and improve materials and components for use in batteries. This research effort supports high-performance rechargeable battery systems, including Li and Li-ion batteries that contain solid-polymer or nonaqueous liquid electrolytes, and MH/NiOOH batteries. Other cross-cutting research efforts are directed at improving the understanding of electrochemical engineering principles, minimizing corrosion of battery components, and analyzing the surfaces of electrodes.

Electrode Characterization studies are an important research element for the successful development of rechargeable electrodes for advanced secondary batteries. Efforts are underway to evaluate the performance of cells utilizing Li-intercalation electrodes, and to use advanced spectroscopic techniques to investigate the chemical state of electrode materials during charge/discharge cycling.

- LBNL used *in situ* ellipsometry to observe detectable changes in the ellipsometry parameters (Δ and Ψ) during the formation of the irreversible surface layer at the carbon/electrolyte interface in 1 M $LiPF_6$ + ethylene carbonate-dimethyl carbonate.
- Lawrence Livermore National Laboratory (LLNL) investigated the Li-intercalation capacities of fluid coke and Santa Maria coke. The capacity for Santa Maria coke ($Li_{0.83}C_6$) is among the highest observed for untreated coke materials.
- The University of Michigan analyzed twelve electrolytes and eleven graphitic materials to determine the quantity and identity of gaseous species produced during initial charge/discharge cycles in Li/C cells. A direct correlation was established between electrochemical capacity and the ratio of basal-plane area to edge area of graphitic materials.
- Brookhaven National Laboratory (BNL) observed by *in situ* extended X-ray diffraction (XRD) and X-ray absorption spectroscopy (XAS) the presence of a third phase during charge of a $LiMn_2O_4$ electrode in 1 M $LiPF_6$/1:1:3 PC:EC:DMC. The charge rate at which the third phase is detected depends on the preparation method and the presence of other transition metal cations.
- Oak Ridge National Laboratory (ORNL) fabricated $LiMn_2O_4$ sheets that have near-theoretical density (4.3 g/cm^3) with 1–5 μm grains using well-milled powders and a small amount of V_2O_5 as a low-temperature sintering aid.

Electrodes for Electrochemical Cells are being developed to identify low-cost metal hydrides for metal-hydride cells and improved metal oxides for electrochemical capacitors.

- BNL determined the crystal structure of $LaNi_{3.55}Co_{0.75}Mn_{0.4}Al_{0.3}$ and its thermal expansion coefficient from 10 to 300 K.
- The University of South Carolina simplified the three-step process for electroless plating of Ni, Ni-P, Co and Co-P to a one-step process, thereby eliminating a costly activation step with palladium and tin chloride to microencapsulate metal hydride electrodes.

- The University of Michigan completed experiments that show that the mechanical and transport properties of cycled substrates in MH/NiOOH cells are measurably and predictably reduced by decreases in material connectivity.
- The University of Wisconsin observed that NiO is a viable electrode material for capacitors when cycled at potentials less than 300 mV *.vs* saturated calomel electrode (SCE). This project has been completed.

Components for Ambient-Temperature Nonaqueous Cells, particularly electrode/electrolyte combinations that improve the rechargeability of these cells, are under investigation.

- LBNL demonstrated greatly improved utilization (in the range of 80-90%) of the active material for the reaction $2\ Li + S \rightarrow Li_2S$, corresponding to Li/S cell capacities of 1350-1500 mAh/g sulfur.
- Cycling studies of $Li_xM_yMnO_2$ (M = Li, Na, K, Rb, Mg, Ba) and the spinel $LiMn_2O_4$ at the State University of New York (Binghamton) showed that the highest capacity after several cycles was obtained when M = K, which provided an intermediate interlayer spacing, and has the most crystalline lattice.
- LBNL measured conductivities as high as 10^{-6} S/cm at 80°C with two-phase nanocomposite mixtures with no added salt or plasticizers, comparable to, or greater than, that of recently developed dry single-ion-conducting polymers.
- LBNL completed a thermal and transport property study of Parel (high-MW PPO)/$LiCF_3SO_3$.
- North Carolina State University observed that the conductivity of composite polymer electrolytes was independent of silica surface chemistry, and decreased only slightly with silica weight fraction. In all cases the conductivity exceeded 10^{-3} S/cm at room temperature.
- Northwestern University developed a simplified model for ionic motion in polyelectrolytes based on locally harmonic vibrational motions and on charge-trapping potentials. An analytic solution for the single-ion motion problem has been found.
- LBNL observed serious corrosion of Al current collectors in Li/polymer batteries during overcharging of three types of cells: (a) Li/V_6O_{13} (composite electrode), (b) Li/TiS_2 (composite electrode), and (c) Li/V_6O_{13} (thin-film electrode).
- Delaware State University reproducibly synthesized 1-ethyl-3-methylimidazolium tetrachloro-aluminate using nonaqueous, inert-atmosphere techniques.

Cross-Cutting Research is carried out to develop mathematical models of electrochemical systems and to address fundamental phenomenological problems; solutions will lead to improved electrode structures and better performance in batteries.

- Short-time experiments with intercalation electrodes at LBNL were fitted by a mathematical model using computer simulations and yielded reasonably constant fundamental diffusion coefficients of the Stephan-Maxwell transport equations.
- LBNL demonstrated superior performance at high current densities in tests of pasted NiOOH electrodes fabricated with surface-modified high-area microfiber Ni substrates.

- Measurements by LBNL indicated that Li reacts with water vigorously even at 160 K with LiOH as the majority reaction product in the presence of excess surface water.

MANAGEMENT ACTIVITIES

During 1997, LBNL managed 12 subcontracts and conducted a vigorous research program in electrochemical energy storage. LBNL staff members attended project review meetings, made site visits to subcontractors, and participated in technical management of various ETR projects. LBNL staff members also participated in the following reviews, meetings, and workshops:

American Chemical Society Meeting, San Francisco, CA, April 11-16, 1997

Metal Hydride/Nickel Oxide Review Meeting, Washington D.C., April 15, 1997

Second International Conference on Spectroscopic Ellipsometry, Charleston, SC, May 1997

191st Meeting of the Electrochemical Society, Montreal, Canada, May 4-9, 1997

EPSCOR Review Meeting, Chantilly, VA, May 19-21, 1997

32nd Intersociety Energy Conversion Engineering Conference, Honolulu, HI, July 27-August 1, 1997

The 1997 Joint International Meeting of the Electrochemical Society and the International Society of Electrochemistry, Paris, France, August 31-September 5, 1997

Advanced Non-Aqueous Battery R&D Workshop, Hunt Valley, MD, October 15-17, 1997

Conference on Electrochemistry of Carbon Allotropes: Graphite, Fullerenes and Diamond, Case Western Reserve University, Cleveland, OH, October 20-22, 1997

Annual Automotive Technology Development Customers' Coordination Meeting, Dearborn, MI, October 27-30, 1997

11th International Solid Sate Ionics Meeting, Honolulu, HI, November 16-21, 1997

Materials Research Society Fall Meeting, Boston, MA, December 1-5, 1997

ACKNOWLEDGMENTS

This work was supported by the Assistant Secretary for Energy Efficiency and Renewable Energy, Office of Advanced Automotive Technologies of the U.S. Department of Energy under Contract No. DE-AC03-76SF00098. The support from DOE and the contributions by the participants in the ETR Program are acknowledged. The assistance of Ms. Susan Lauer for coordinating the publication of this report and Mr. Garth Burns for providing the financial data are gratefully acknowledged.

ANNUAL REPORTS

1. Exploratory Technology Research Program for Electrochemical Energy Storage – Annual Report for 1996, LBNL-40267 (June 1997).

2. Exploratory Technology Research Program for Electrochemical Energy Storage – Annual Report for 1995, LBNL-338842 (June 1996).

3. Exploratory Technology Research Program for Electrochemical Energy Storage – Annual Report for 1994, LBL-37665 (September 1995).

4. Exploratory Technology Research Program for Electrochemical Energy Storage – Annual Report for 1993, LBL-35567 (September 1994).

5. Exploratory Technology Research Program for Electrochemical Energy Storage – Annual Report for 1992, LBL-34081 (October 1993).

6. Exploratory Technology Research Program for Electrochemical Energy Storage – Annual Report for 1991, LBL-32212 (June 1992).

7. Technology Base Research Project for Electrochemical Energy Storage – Annual Report for 1990, LBL-30846 (June 1991).

8. Technology Base Research Project for Electrochemical Energy Storage – Annual Report for 1989, LBL-29155 (May 1990).

9. Technology Base Research Project for Electrochemical Energy Storage – Annual Report for 1988, LBL-27037 (May 1989).

10. Technology Base Research Project for Electrochemical Energy Storage – Annual Report for 1987, LBL-25507 (July 1988).

11. Technology Base Research Project for Electrochemical Energy Storage – Annual Report for 1986, LBL-23495 (July 1987).

12. Technology Base Research Project for Electrochemical Energy Storage – Annual Report for 1985, LBL-21342 (July 1986).

13. Technology Base Research Project for Electrochemical Energy Storage – Annual Report for 1984, LBL-19545 (May 1985).

14. Annual Report for 1983 – Technology Base Research Project for Electrochemical Energy Storage, LBL-17742 (May 1984).

15. Technology Base Research Project for Electrochemical Energy Storage – Annual Report for 1982, LBL-15992 (May 1983).

16. Technology Base Research Project for Electrochemical Energy Storage – Report for 1981, LBL-14305 (June 1982).

17. Applied Battery and Electrochemical Research Program Report for 1981, LBL-14304 (June 1982).

18. Applied Battery and Electrochemical Research Program Report for Fiscal Year 1980, LBL-12514 (April 1981).

LIST OF ACRONYMS

AES	Auger electron spectroscopy
ATR	attenuated total reflectance
BNL	Brookhaven National Laboratory
DEC	diethyl carbonate
DLE	discrete lattice expansion
DMC	dimethylcarbonate
DME	dimethoxyethane
DOE	Department of Energy
DSC	differential scanning calorimetry
EC-DMC	ethylene carbonate-dimethyl carbonate
EDX	energy dispersive X-ray analysis
EMA	effective medium approximation
EPRI	Electric Power Research Institute
ESCA	electron spectroscopy for chemical analysis
ETR	Exploratory Technology Research
EV	electric vehicle
EXAFS	extended X-ray absorption fine structure
FWHM	full width half maximum
GPC	gel permeation chromatography
HEV	hybrid electric vehicle
HOPG	highly ordered pyrolytic graphite
HRTEM	high-resolution transmission electron microscopy
IECEC	Intersociety Energy Conversion Engineering Conference
IR	infrared
ISE	International Society of Electrochemistry
LBNL	Lawrence Berkeley National Laboratory
Lipon	lithium phosphorous oxygen nitrogen
LLNL	Lawrence Livermore National Laboratory
LRB	lithium rechargeable battery
NIST	National Institute of Standards and Technology
NMR	nuclear magnetic resonance
NSLS	National Synchrotron Light Source
ORNL	Oak Ridge National Laboratory
PC	propylene carbonate
PDI	polydispersity indices
PEG-DME	polyethylene glycol - dimethyl ether
PEO	poly(ethylene oxide)
PNGV	Partnership for a New Generation of Vehicles
PPO	polydimethylphenylene oxide

SCE	saturated calomel electrode
SEI	solid electrolyte interface
SEM	scanning electron microscopy
SERS	surface-enhanced Raman spectroscopy
TEM	transmission electron microscopy
TGA	thermogravimetric analysis
THF	tetrahydrofuran
TMA	tetramethyl ammonium
UHV	ultrahigh vacuum
USABC	United States Advanced Battery Consortium
VTF	Vogel-Tamman-Fulgher
XANES	X-ray absorption near-edge spectroscopy
XAS	X-ray absorption spectroscopy
XPS	X-ray photoelectron spectroscopy
XRD	X-ray diffraction

SUBCONTRACTOR FINANCIAL DATA - CY 1997

Subcontractor	Principal Investigator	Project	Contract Value (K$)	Term (months)	Expiration Date	Status in CY 1997*
Electrode Characterization						
Lawrence Berkeley National Laboratory	E. Cairns, L. DeJonghe, J. Evans, J. Kerr, K. Kinoshita, F. McLarnon, J. Newman, P. Ross	Electrochemical Energy Storage	1715	12	9-98	C
Lawrence Livermore National Lab.	T. Tran	Li-Ion Carbon Electrode	75	12	12-98	C
University of Michigan	G. Nazri	Carbonaceous Anodes	140	12	9-98	C
Brookhaven National Laboratory	J. McBreen	Battery Materials				C
Oak Ridge National Laboratory	J. Bates	Rechargeable Li Batteries				T
Electrodes for Electrochemical Cells						
Brookhaven National Laboratory	J. Reilly	Metal Hydride Electrodes				C
University of South Carolina	R. White	Metal Hydride Properties	90	12	8-97	C
University of Michigan	A.M. Sastry	Novel Cell Components	134	12	9-98	C
University of Wisconsin	M. Anderson	Sol-Gel Derived Metal Oxides	123	12	8-97	T
Components for Ambient-Temperature Nonaqueous Cells						
SUNY at Binghamton	S. Whittingham	Cathode Materials	65	12	5-99	C
North Carolina State University	S. Khan	Polymer Electrolytes	100	12	9-98	C
Northwestern University	M. Ratner	Polymer Electrolytes	100	12	12-98	C
Delaware State University	K. Wheeler	Transition-Metal Oxides	90	13	3-98	C

* C = continuing, T = terminating

INTRODUCTION

This report summarizes the progress made by the Exploratory Technology Research (ETR) Program for Electrochemical Energy Storage during calendar year 1997. The primary objective of the ETR Program, which is sponsored by the U.S. Department of Energy (DOE) and managed by Lawrence Berkeley National Laboratory (LBNL), is to identify electrochemical technologies that can satisfy stringent performance, durability and economic requirements for electric vehicles (EVs) and hybrid-electric vehicles (HEVs). The ultimate goal is to transfer the most-promising electrochemical technologies to the private sector or to another DOE program for further development and scale-up. Besides LBNL, which has overall responsibility for the ETR Program, BNL, LLNL and ORNL participate in the ETR Program by providing key research.

The various project objectives, research activities and accomplishments are presented in the technical summaries that follow. Financial information and a description of the management activities for the ETR Program are described in the Program Summary.

RESEARCH PROJECT SUMMARIES

ELECTRODE CHARACTERIZATION

Characterization of electrode morphology and chemical composition are important for the successful development of rechargeable electrodes for advanced secondary batteries. Efforts are underway to utilize advanced microfabrication techniques and spectroscopy to characterize electrode properties.

Carbon Electrochemistry

Kim Kinoshita
90-1142, Lawrence Berkeley National Laboratory, Berkeley CA 94720
(510) 486-7389; fax: (510) 486-4260; e-mail: k_kinoshita@lbl.gov

Objective

- Identify the critical parameters that control the reversible intercalation of Li in carbonaceous materials and determine their maximum capacity for Li intercalation.

Approach

- Couple electrochemical studies with physical measurements to correlate the relationship between the physicochemical properties of carbonaceous materials and their ability to intercalate Li.

Accomplishments

- An electrochemical cell was fabricated and used for *in situ* ellipsometry studies of the carbon/electrolyte interface in 1 M $LiPF_6$ + ethylene carbonate-dimethyl carbonate (ED-DMC). Detectable changes in the ellipsometry parameters (Δ and Ψ) were measured at potentials near 1.5 V, where a high cathodic current on a carbon film electrode was observed.

Future Directions

- Characterize the properties of heat-treated petroleum cokes and identify the appropriate precursor to form more-spherical carbon particles.
- Continue *in situ* ellipsometry studies of lithiated carbons, and determine the relationship between the type of carbon and the properties of the surface layer formed during the first charge cycle.

The objective of this project is to identify the critical parameters that control the reversible intercalation of Li in carbonaceous materials. This project investigates the role of physicochemical properties of carbonaceous materials in their ability to reversibly intercalate Li. This latter effort is coordinated with the research conducted at LLNL to evaluate the intercalation of Li in carbonaceous materials for rechargeable Li batteries (see discussion in "Fabrication and Testing of Carbon Electrodes as Lithium Intercalation Anodes").

The collaboration with Superior Graphite (Chicago, IL) and LLNL continued with the focus to evaluate alternative graphitized carbons for the negative electrodes in Li-ion cells. The goal of the current experiments is to identify graphitized carbon particles which are more spherical in shape and with a higher charge/discharge rate capability. A variety of different cokes was received from Superior Graphite for evaluation in Li-ion cells. After discussion with LLNL and Superior Graphite it was decided to heat treat several of the cokes at 1800 and 2300°C to determine the influence of heat treatment on the carbon morphology and Li storage capacity. A calcined fluid coke, with a more spherical particle shape, was heat treated at these two temperatures for one hour in nitrogen. These studies will complement the previous findings with heat treatment of a petroleum needle coke.

X-ray diffraction (XRD) analysis of the calcined fluid coke indicated that the (002) d-space decreased from 3.470 Å (original without heat treatment) to 3.458 Å (1800°C) and 3.431 Å (2300°C). Transmission electron microscopy (TEM) of these fluid coke samples showed significant changes in the lattice image as the heat-treatment temperature was increased to 2300°C. The original calcined fluid coke showed only short-range ordering of the lattice planes, similar to that of petroleum cokes.

Other studies underway in this project are to reduce the irreversible capacity loss during the first potential scan to form lithiated carbons, and to investigate the properties of the surface film that forms. An electrochemical cell was fabricated and used for *in situ* ellipsometry studies of the carbon/electrolyte interface during potential cycling in nonaqueous electrolytes. The initial studies were conducted on smooth carbon films obtained by pyrolysis of a positive photoresist on a Si wafer at 1000°C. The potential of the carbon film in 1 M $LiPF_6$ + EC-DMC was scanned from open circuit (3.0 V) to 0 V (*vs.* Li), and the ellipsometry parameters Δ and Ψ were recorded (Fig. 1). Detectable changes in the ellipsometry parameters occurred during the first scan at potentials near 1.5 V, where a large cathodic current was observed (Fig. 2). These changes are attributed to the formation of a solid electrolyte interface (SEI) layer. Subsequent potential scans between 3.0 and 0 V showed no significant change in the ellipsometry parameters or the current-potential profiles, indicative of a SEI layer which remained unchanged. X-ray photoelectron spectroscopy measurements indicated that Li and F were the major elements present in the SEI layer on the carbon surface. Preliminary analysis of the ellipsometry data using a single-layer effective medium approximation (EMA) model indicated that the SEI layer was 4 nm thick.

PUBLICATIONS

T.D. Tran L.M. Spellman, W.M. Goldberger, X. Song and K. Kinoshita, "Lithium Intercalation in Heat-Treated Petroleum Cokes," *J. Power Sources* **68**, 106 (1997).

T.D. Tran, L.C. Murguia, X. Song and K. Kinoshita, "Lithium Intercalation Behavior of Surface-Modified Carbonaceous Materials," in *Proc. of the Symposium on Batteries for Portable Applications and Electric Vehicles*, Vol. 97-18, C. Holmes and A. Landgrebe, eds. The Electrochemical Society, Inc., Pennington, NJ (1997) p. 82.

R. Kostecki, T. Tran, X.Y. Song, K. Kinoshita and F. McLarnon, "Raman Spectroscopy and Electron Microscopy of Heat-Treated Petroleum Cokes for Lithium-Intercalation Electrodes," *J. Electrochem. Soc.* **144**, 3111 (1997).

F. Kong, J. Kim, X. Song, M. Inaba, K. Kinoshita and F. McLarnon, "Exploratory Studies of the Carbon/Nonaqueous Electrolyte Interface by Electrochemical and *In Situ* Ellipsometry Measurements," LBNL-41097 (November 1997), accepted for publication, *Electrochemical and Solid State Letters* (1998).

K. Kinoshita, "Advanced Anode Materials for Li-Ion Batteries," LBNL-40721 (October 1997), in *New Trends in Electrochemical Technology: Energy Storage Systems for Electronics*, M. Datta, ed., Gordon and Breach Science Publishers, London, U.K.

D. Derwin, K. Kinoshita, T.D. Tran and P. Zaleski, "Commercial Cokes and Graphites as Anode Materials for Lithium-Ion Cells," Materials Research Society Fall Meeting, Boston, MA. December 1-5, 1997, paper Y10.10, in *Proc. of the Symposium on Materials for Electrochemical Energy Conversion and Storage II - Batteries, Capacitors and Fuel Cells*, Volume 496, D. Doughty, D. Ginley, B. Scrosati, T. Takamura and J. Zhang, eds., Materials Research Society, Warrendale, PA (1997).

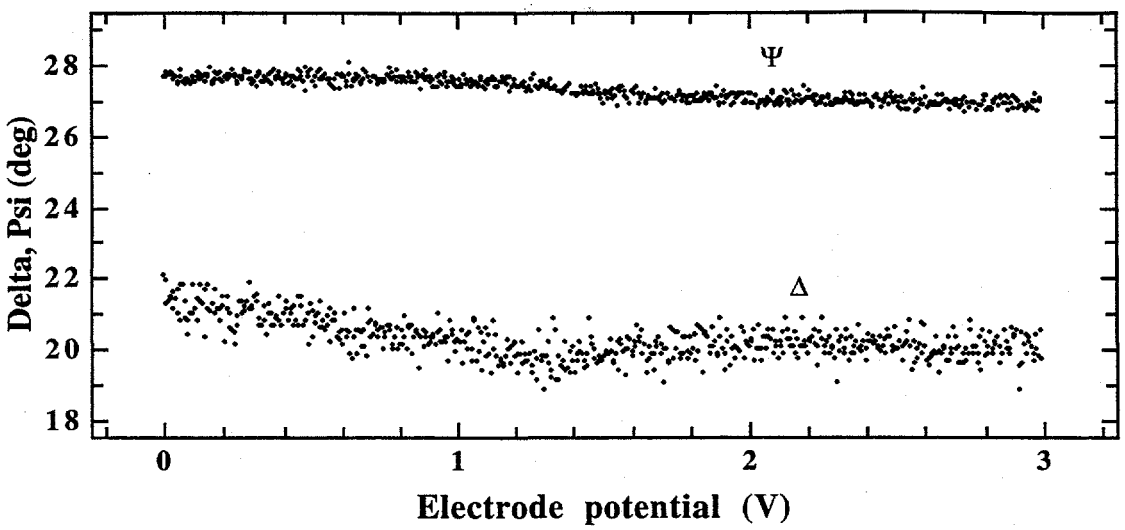

Figure 1. Cyclic voltammograms of carbon film electrode in 1 M $LiPF_6$/EC-DMC. Scan rate is 5 mV/s.

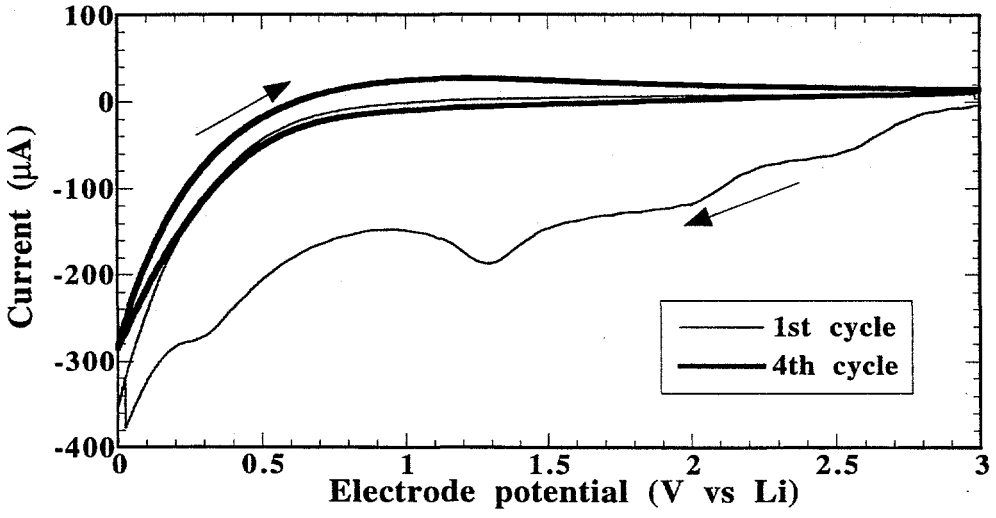

Figure 2. Ellipsometry parameters (Δ and Ψ) measured at a wavelength of 500 nm during the initial cathodic potential scan from 3.0 to 0 V.

Fabrication and Testing of Carbon Electrodes as Lithium-Intercalation Anodes

Tri D. Tran
L-322, Lawrence Livermore National Laboratory, P.O. Box 808, Livermore CA 94550
(925)422-0915; fax: (925) 423-4897; e-mail: tran4@llnl.gov

Objectives

- Evaluate the performance of carbonaceous materials as hosts for Li-intercalation negative electrodes.
- Develop reversible Li-intercalation negative electrodes for advanced rechargeable Li-ion cells.

Approach

- Fabricate electrodes from various commercial carbons and graphites and evaluate in small Li-ion cells.
- Correlate electrode performance (*i.e.*, capacity, irreversible capacity) with carbon structure and properties in collaboration with LBNL.

Accomplishments

- The Li intercalation capacities of fluid coke and the Santa Maria coke were found to have x-values (in Li_xC_6) of 0.65 and 0.83, respectively. The capacity for Santa Maria coke is among the highest observed for untreated coke materials.

Future Direction

- Continue evaluation of commercial and chemically-modified carbon materials for Li intercalation.

Two types of graphitizable and commercial petroleum cokes from Superior Graphite Company were investigated as electrode materials for Li intercalation. They include a standard fluid coke and a Santa Maria (fluid) coke. The fluid coke materials consist of spherical grains with a spherical layer structure and are generally less graphitizable than the needle-type cokes which we studied last year. They are expected to provide smoother and more-rounded particles, yielding potentially low capacity loss and high rate capability. In contrast, needle cokes with a preferred microstructural orientation tended to form platelet-like structures with a large fraction of active surfaces. The surface morphology of the final particles has been found to affect their performance.

The cokes were heat treated in an inert atmosphere at temperatures between 1400 to ~2800°C. The raw materials and graphitized materials (~2800°C) were commercial products from Superior Graphite Co. The raw cokes were further treated at two intermediate temperatures of 1800 and 2300°C at LBNL. The materials were fabricated into electrodes using a carbon-based phenolic resin binder. This electrode fabrication procedure has been described earlier. The materials were studied in 0.5 M HQ115/EC/DMC (50/50) electrolytes. Table 1 shows the physical characteristics and electrochemical performance of these materials. Data for a series of needle cokes are also included for comparison.

The reversible capacities observed with the fluid coke and the Santa Maria coke correspond to x-values (in Li_xC_6) of 0.65 and 0.83, respectively. The capacity for Santa Maria coke is among the highest observed for untreated coke materials. The potential profiles of these materials exhibit gradual changes with Li concentration, consistent with those obtained with amorphous carbons. The irreversible capacity loss associated with the formation of the SEI are 127 and 178 mAh/g, respectively. The reversible capacities decreased for the samples treated at 1800 and 2300°C. The capacities for the graphitized samples (heat treated at ~2800°C) increase but are significantly lower than that associated with graphite (LiC_6). The potential profiles, however, show graphite-like features. The irreversible capacities decrease with increasing heat treatment temperature, parallel with a decrease in surface areas (Table 1).

Figure 3 compares the plots of the reversible capacities versus d_{002} spacing for the two fluid cokes and that of the needle coke (LS190, Superior Graphite). The increasing heat treatment temperatures resulted in graphitization of the

structure as reflected in the decreasing stack spacing (Table 1). The reversible capacities show a minimum which appears at a d_{002} spacing of about 3.43 Å, which is consistent with published data. The significance of the results and additional characterization are the subject of our current research.

Table 1. Physical properties and performance of petroleum cokes of different morphology

Sample	Particle size (mm)	d_{002} (Å)	BET area (m^2/g)	Reversible capacity (x, Li_xC_6)	Irreversible capacity (mAh/g)
Fluid coke					
as-received	22	3.470	6.8	0.65	127
1800°C	22	3.458	2.8	0.48	82
2300°C	22	3.431	1.5	0.55	73
~2800°C	25	3.399	5.1	0.60	100
SantaMaria coke					
as-received	11	3.489	11.2	0.83	178
1800°C	11	3.436	4.8	0.6	100
2300°C	11	3.390	3.1	0.62	61
~2800°C	21	3.377	8.0	0.84	100
Needle coke (LS190)					
as-received	30-40	3.442	0.4	0.69	65
1800°C	10	3.410	5.6	0.45	81
2100°C	10	3.359	4.6	0.74	110
2350°C	10	3.358	4.3	0.81	130

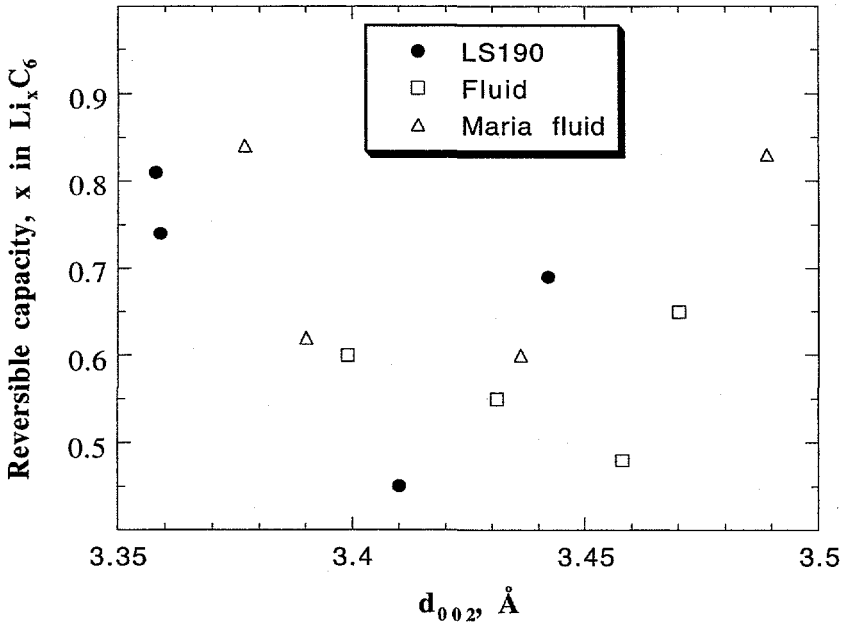

Figure 3. Plots of reversible capacities *vs.* d_{002} spacing

Reactivity and Safety Aspects of Carbonaceous Anodes Used in Lithium–Ion Batteries

*M. David Curtis and Gholam-Abbas Nazri**
Department of Chemistry, University of Michigan, Ann Arbor MI 48109-1055
**Physics and Physical Chemistry Department, GM Research and Development Center, Warren, MI 48090*
(734) 763-2132; fax: (734) 763-2307; e-mail: mdcurtis@umich.edu / gnazri@cmsa.gmr.com

Objectives

- Identify and quantify the gaseous products generated at carbonaceous electrodes during initial charge/discharge cycles in Li-ion batteries.
- Establish structure-electrochemical property relationships of various carbonaceous materials.

Approach

- Employ GC/MS to analyze gases produced in test cells as a function of electrolyte composition and nature of carbonaceous material.
- Apply spectroscopic/analytic techniques (XRD, Raman, IR spectroscopy) to characterize carbon and surface films formed during initial charge/discharge cycles.

Accomplishments

- Twelve electrolytes and eleven graphitic materials were analyzed to determine the quantity and identity of gaseous species produced during initial charge/discharge cycles
- A direct correlation was established between electrochemical capacity and ratio of basal-plane area to edge area of graphitic materials.

Future Directions

- Extend measurements to sub-ambient and elevated temperatures.
- Examine effect of surface treatment of graphitic material on nature and quantity of evolved gases.
- Conduct differential scanning calorimetry (DSC) analysis of Li-doped graphitic anodes as a function of doping level.

The objective of this project is to measure and identify the gaseous species generated on carbonaceous electrodes in Li-ion batteries during initial charge-discharge cycles, and to determine the relationship between the carbon structure — electrolyte composition and the type of generated gases. This effort is directed at the fabrication and characterization of Li/C cells with various *in situ* and *ex situ* techniques to investigate the abuse tolerance and reactivity of various carbonaceous electrodes.

In this work we analyzed the gaseous species generated on carbonaceous anodes using *in situ* mass spectrometry and IR spectroscopy. Electrochemical cells were fabricated with carbonaceous electrodes (100 cm^2 area) and metallic Li electrodes in liquid electrolytes with various solvent and salt compositions. An Arbin battery cycler was used for electrochemical testing and a MacPile cycler was employed for *in situ* X-ray diffraction and IR spectroscopy of 2.5 cm^2 cells. The identity of the solid films formed on carbonaceous anodes during the initial charge-discharge cycles was also established using IR spectroscopy. The structural parameters of various graphitic materials were determined using X-ray diffraction and Raman spectroscopy. The particle morphology, size and shape of graphitic materials were analyzed using scanning electron microscopy (SEM).

The composition of gaseous species generated at various carbonaceous electrodes as a function of electrolyte compositions is listed in Table 2. With most low-surface-area graphitic electrodes, more than 90% of the gases are generated during the first Li-intercalation process. However, high-surface-area carbonaceous electrodes continued producing gases even up to 5-7 cycles. The nature of the gaseous species generated on carbonaceous electrodes is highly dependent on the nature and origin of the graphitic material when the cell

Table 2. Nature of gaseous species formed on carbonaceous electrodes during initial charge-discharge cycles as function of electrolyte composition and graphite structure.

		Generated gases during the first few cycles (volume ml/g of graphite)											
Graphite	Electrolytes	CO	O_2	C_2H_4	CH_4	H_2O	C_2H_4O	H_2	C_2H_6	C_3H_6	C_3H_4	C_3H_8	Vol_{tot} (ml/g)
BG-35	EC-DEC	35.58	29.14	3.15	0	1.78	0.68	3.63	0	0	0	0	73.96
	EC-PC	-	-	-	-	-	-	-	-	-	-	-	-
	EC-DMC	20.36	21.37	0	2.77	2.31	4.49	3.52	1.59	0	0	0	56.39
	PC	21.24	26.77	3.33	0.53	0.48	1.54	4.70	5.33	16.95	6.57	0	87.44
CPC	EC-DEC	5.79	10.38	22.85	0	1.54	0.56	1.21	0.30	0	0	0	42.63
	EC-PC	16.77	7.47	7.47	0.19	0	0	2.25	0	4.71	4.66	0	43.52
	EC-DMC	20.01	24.72	7.88	3.30	1.36	5.32	2.52	0	0.88	0	0	66.19
	PC	18.81	28.49	8.29	0	0	1.94	4.27	0	19.13	7.55	0	88.48
CN-39	EC-DEC	7.99	14.42	21.37	0.86	0.71	2.86	0.86	0	0	0	0	49.05
	EC-PC	10.02	7.63	9.18	0	0.30	0	2.83	0	6.87	3.50	0	40.33
	EC-DMC	10.08	6.38	7.63	2.63	0.94	3.51	1.05	0	2.90	0	0	35.10
	PC	19.70	34.16	17.40	0	0.70	1.49	4.61	12.80	27.45	16.15	0	134.46
CN-39A	EC-DEC	8.66	7.86	7.31	0	0.35	0	0.86	0	0	0	0	25.04
	EC-PC	40.29	31.98	0.53	0.41	4.22	0.77	8.31	1.25	0.48	0	2.53	90.77
	EC-DMC	18.32	16.26	10.73	1.24	0.67	2.35	2.00	2.28	0.71	0	0	54.56
	PC	45.86	47.12	0	1.48	0.86	3.46	3.16	1.28	2.18	0	0	105.4
KS-44	EC-DEC	7.54	5.74	6.99	0	0.30	0	3.34	0	0	0	0	23.91
	EC-PC	21.31	28.49	8.86	0	0.78	0.67	5.14	0.56	8.15	0	0	73.96
	EC-DMC	11.95	10.43	7.60	3.14	0	3.09	2.29	0	0	0	0	38.50
	PC	12.14	22.88	3.64	0.27	0.33	0.49	2.16	7.17	15.79	9.44	0	74.31
SFG-15	EC-DEC	0	7.50	30.54	0	0	2.05	0.49	0	0	0	0	40.58
	EC-PC	25.54	22.86	14.22	0	0.40	0.29	2.87	0.74	9.86	0	0	76.78
	EC-DMC	12.22	11.27	2.10	0	0.70	0.15	1.81	0	0	0.28	0.63	29.16
	PC	23.08	31.76	4.32	0.96	0.44	0.96	6.48	8.32	26.44	11.28	0	114.04
BG-34	EC-DEC	10.23	12.96	24.29	0	2.33	0	2.09	0	0	0	0	51.9
	EC-PC	17.57	38.48	29.46	0	0.44	1.64	6.22	0	34.78	0	0	128.59
	EC-DMC	5.28	13.88	7.85	1.19	0.39	0.78	2.16	0	0	0	1.00	32.53
	PC	25.74	34.10	8.44	1.14	0.86	0.98	2.18	0	22.66	12.46	0	108.56

voltage is maintained above that for electrode decomposition, E>0.85 V. However, at voltages <0.85 V, the nature of gases is sensitive to the composition of electrolytes. The amount of gaseous species generated above the electrolyte decomposition voltage are highly dependent on the purity of the carbon and the nature of the functional groups on the carbon surface, including trapped moisture. In general, the amount of gaseous species generated above the electrolyte decomposition voltage is a fraction of the total gases produced during electrolyte decomposition, (about 1-5 vol%).

XRD analysis of crystal parameters, L_a and L_c, and degree of graphitization (FWHM) correlate well with higher electrochemical capacity. A better correlation was found between the electrochemical capacity and the ratio of graphitic peak to non-graphitic peak of the Raman spectra, I_g/I_d. We have found that Raman spectra provide a better representation of the defects in graphites than the XRD data. Raman spectra also provide a better correlation with the electrochemical performances of graphitic materials.

Thermal analysis of carbonaceous electrodes at various degrees of Li doping and further analysis of solid films formed on the carbonaceous electrodes in different organic electrolytes are also in progress.

PUBLICATION

G.A. Nazri, B. Yebka, M. Nazri, M.D. Curtis, K. Kinoshita and D, Derwin, "Safety and Reactivity of Carbonaceous Anodes in Lithium Battery Technology," *193rd Meeting of the Electrochemical Society*, San Diego, CA, May 3-8, 1998.

Battery Materials: Structure and Characterization

James McBreen
Brookhaven National Laboratory, DAS-Bldg. 480, P.O. Box 5000, Upton NY 11973-5000
(516) 344-4513,;fax: (516) 344-4071; e-mail: mcbreen@bnlarm.bnl.gov

Objective

- Elucidate the molecular aspects of battery materials and processes by *in situ* synchrotron X-ray techniques.

Approach

- Apply extended X-ray absorption fine structure (EXAFS) to the study of Li_xCoO_2, Li_xNiO_2 and $Li_xMn_2O_4$ electrodes.

Accomplishments

- Combined *in situ* XRD and X-ray absorption spectroscopy (XAS) studies were used to study mixed cation oxides in rechargeable Li cells.
- The role of both transition metals in mixed-cation oxides was elucidated for Ni and Cu substituted manganese spinels.

Future Direction

- Use *in situ* XRD and XAS to study the cycling behavior and failure mechanisms of Li intercalation electrodes, including metal oxides with two transition elements.

The objective of this research is to elucidate the molecular aspects of materials and electrode processes in advanced rechargeable Li batteries and to use this information to develop electrode and electrolyte structures with low cost, good performance, and long life. Work during the year included both *in situ* high-resolution XRD and EXAFS studies on cathodes for Li batteries.

***In Situ* XAS Studies of $LiNiO_2$ Electrodes.** XAS results on $LiNiO_2$ showed that each Ni was coordinated with four O atoms at a distance of 1.91Å and two O atoms at a distance of 2.09 Å. This is at variance with analysis of previously reported XRD results, which gave an octahedral coordination of six O atoms with a Ni-O distance of 1.969Å. However, in agreement with the XRD results, the XAS shows that the coordination in the Ni-Ni second shell is symmetrical, with a Ni-Ni bond distance of 2.9 Å. In the *in situ* study, the pre-edge and edge features of the XAS spectra indicate that the oxidation change on the Ni is not from +3 to +4. The results are more consistent with an oxidation change of the Ni, during charge, from ca. 2.4-2.5 to ca. 3.3-3.4, a behavior similar the α-$Ni(OH)_2/\gamma$-NIOOH couple. This was explained by invoking a charge-compensation mechanism based in part on holes residing on the oxygen atom sites. The EXAFS showed that during charge there was an increase in the contribution of the short Ni-O coordination with the coordination exceeding five, and the short bond distance decreasing from 1.92 to 1.88 Å. At the end of charge there was a residual contribution from the longer bond distance at 2.1 Å, with the coordination number decreasing to less than one. On charge the Ni-Ni bond distances decreased from 2.9 to 2.83 Å. The EXAFS showed that the disorder associated with the Ni-Ni atom pair increased until half of the Li was removed and then decreased for the rest of the charge. The disorder may be associated with the intermediate monoclinic phase. The hexagonal phases that exist at the beginning and end of charge are more ordered.

***In Situ* High-Resolution XRD Studies of $LiMn_2O_4$ Cathodes.** An X-ray diffraction beam line at the National Synchrotron Light Source (NSLS) was used for *in situ* XRD studies on several $LiMn_2O_4$ cathode materials. The materials included six obtained from commercial suppliers, and others prepared at BNL by conventional thermal methods and the Pechini method. A sample obtained from E. Merck (Darmstadt, Germany) was cycled in a $Li/Li_xMn_2O_4$ cell with a 1 M $LiPF_6$ electrolyte in a 1:1:3 PC:EC:DMC solvent. XRD results showed the appearance of a second cubic phase during the first charge. On the second cycle a third cubic phase was detected. The results for the second cycle are shown in Figs. 4 and 5. As the cell was charged at the C/20 rate, diffraction patterns were obtained continuously (25 min/scan)

over a range that included the (511), (440) and (531) reflections. The appearance of a second phase (Phase II) at about 60% of charge has been previously reported. However, this is the first time that the appearance of a third phase (Phase III) at about 40% charge has been observed. Our most recent work shows that formation of Phase II is suppressed in stoichiometries with excess Li. However, there is line broadening in the charge region where this phase normally appears. This indicates that formation of Phase II is suppressed but not completely eliminated. If the charge rate is low enough Phase III is seen in all materials. The charge rate at which Phase III can be detected depends on the preparation method and the presence of other transition metal cations.

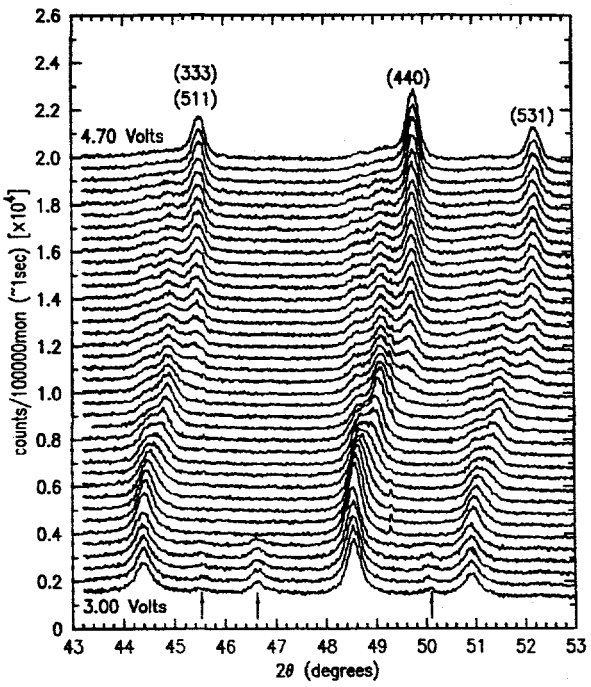

Figure 4. XRD patterns for Merck $LiMn_2O_4$ during second charge: discharged state, bottom; charged state, top.

X-ray Studies of Mixed Oxides. *In situ* X-ray absorption studies were carried out on several $Li_xMn_2O_4$ oxides with substitutions of Ni and Cu and with combinations of Ni and Cu. These materials were prepared by Covalent Associates, Inc. by a sol-gel method. The $Li_xNi_{0.5}Mn_{1.5}O_4$ spinel is interesting because it does not undergo a tetragonal distortion on the 3 V plateau [Amine et al., *J. Electrochem. Soc.* **143**, 1607 (1996)] and it displays a higher voltage plateau at 4.7 V [Zhong et al., *ibid.*, **144**, 205 (1997)]. The XAS results on the as-prepared material were consistent with the presence of only Mn(IV) species and the compound has the formula $LiNi(II)_{0.5}Mn(IV)_{1.5}O_4$. During charge at the 4.7 V plateau there was no change in the Mn oxidation state. However the Ni was oxidized from Ni(II) to a higher valence state. *In situ* XRD showed that the presence of Ni enhanced the formation of Phase II and Phase III on the 4.7 V plateau. On the 3 V plateau the formation of the tetragonal phase was suppressed even with repeated cycling.

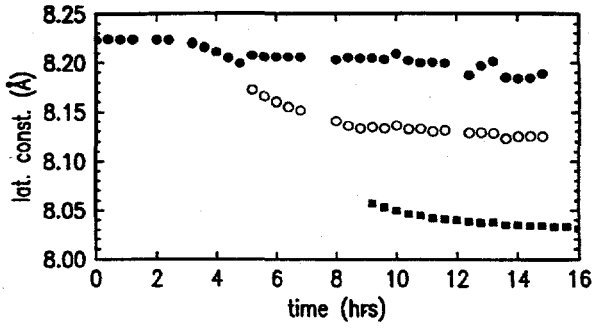

Figure 5. Lattice constants for cubic phases occurring on second charge.

Both *in situ* XAS and XRD were carried out on a mixed oxide, $LiCu_{0.5}Mn_{1.5}O_4$ that was cycled in a cell with a 1 M $LiPF_6$ electrolyte in an EC/DMC solvent. The cell exhibited two voltage plateaus, one at 4.1 V, the other at 4.9 V. The X-ray absorption near-edge structure (XANES) results at the Cu and Mn K edges indicate that on the lower plateau residual Mn(III) is oxidized to Mn(IV). On the upper plateau Cu(II) is oxidized to Cu(III). *In situ* XRD shows single-phase behavior, with no formation of either Phase II or Phase III throughout charge. There is a contraction of the lattice on the lower plateau. On the upper plateau the lattice constant does not vary.

PUBLICATION

J. McBreen, S. Mukerjee, X.Q. Yang, T.R. Thurston and N.M. Jisrawi. "*In situ* Synchrotron X-ray Studies of $LiMn_2O_4$ Cathodes," *Proc. 2nd. Int. Symp. On New Materials for Fuel Cells and Modern Battery Systems*, O. Savadogo and P. R. Roberge, eds., pp. 348-357, Ecole Polytechnique de Montréal, Montreal, Canada, July 6-10, 1997.

Development of a Thin-Film Rechargeable Lithium Battery for Electric Vehicles

John B. Bates
MS 6030, Oak Ridge National Laboratory, P.O. Box 2008, Oak Ridge TN 37830-6030
(615) 574-6280; fax: (615) 574-4143; e-mail: joh@ornl.gov

Objectives

- Develop solid-state Li-$Li_xMn_2O_4$ rechargeable batteries for EV applications that meet or exceed the long-term goals of the USABC.

Approach

- Fabricate $LiMn_2O_4$ ceramic sheets < 50 μm-thick by tape-casting and sintering techniques which are near theoretical density with a very fine and homogeneous grain structure.
- Fabricate and cycle test hybrid batteries formed by vapor deposition of the Lipon electrolyte, Ni current collector, and Li anode.

Accomplishment

- $LiMn_2O_4$ sheets near theoretical density (4.3 g/cm^3) with 1–5 μm grains have been fabricated using well-milled powders and a small amount of V_2O_5 as a low-temperature sintering aid.

Future Directions

- Project has been completed.

The objective of this project is to fabricate all-solid-state batteries that utilize the thin-film 'Lipon' solid electrolyte developed at ORNL. This sputter-deposited electrolyte is stable indefinitely for thin-film batteries cycled at 100°C up to voltages of 4.5 V with $LiMn_2O_4$ and metallic Li electrodes. For a successful battery, the Lipon must be deposited onto a cathode with a dense smooth surface which is stable in the plasma environment. To maximize the energy and power densities, a single-phase $LiMn_2O_4$ cathode must be 30–50 μm thick and preferably in the form of a freestanding ceramic sheet.

We are fabricating $LiMn_2O_4$ cathodes by tape-casting techniques. Earlier attempts to fabricate tape-cast and sintered sheets, 30–150 μm-thick, resulted in tapes with densities up to 90%, but with very large grains and pores(10–50 μm). Batteries fabricated with these tapes showed poor cyclability and a limited capacity presumably due to the weak grain boundaries and stress induced by the volume change accompanying the Li intercalation/deintercalation reaction. We believed that a high-density tape with much finer grains would have both higher strength and better electrochemical properties.

During this year, several approaches were pursued to fabricate fine-grained $LiMn_2O_4$ tapes: (i) The slip was reformulated to increase the solid loading. (ii) The green tapes were compacted by cold pressing and roller compaction. (iii) The commercial $LiMn_2O_4$ powders were aggressively milled utilizing ball, attrition, and jet-milling techniques. (iv) Slips were formulated with V_2O_5, which melts at 690°C, as a sintering aid. (v) Ultrafine, high-purity powders were synthesized by sol-gel techniques. Both (i) and (ii) led to a higher sintered density, but the grains and pores were still quite large. Addition of the sintering aid (iv) lowered the sintering temperature from 1150 to 700°C, and for tapes made with well-milled powders (iii), the grain size was reduced to 1-5 μm. The greatly improved microstructure of the sintered $LiMn_2O_4$ tapes is shown in Fig. 6. These tapes are near the theoretical density, ~4.3 g/cm^3. (Tapes using the sol-gel powders have not been fabricated.)

Solid-state batteries were fabricated with these fine-grained sintered tapes by vapor deposition of the remaining battery components, Lipon, Ni and Li. Unfortunately, persistent difficulties were encountered with cycling the batteries at both 100 and 25°C. Although ac impedance and pulse testing indicate that, at least initially, the cathode and interface resistivities are quite low, the batteries developed high polarization, particularly in the discharge mode, after a short time under test. Typically upon the

polarization, particularly in the discharge mode, after a short time under test. Typically upon the initial charge, about 25% of the Li is readily deintercalated, and the cell voltage follows the expected increase along the 4-V plateau. However, on discharge to a 3- or 2.5-V cutoff, only a small fraction of the expected capacity is recovered. An example of shorter stepwise charge/discharge tests is shown in Fig 7. Even after short charge cycles, only a fraction of the expected capacity is obtained upon discharge due to high polarization. Extending the discharge to lower voltages was avoided because of the potentially deleterious tetragonal lattice distortion. Examination of these cathodes by SEM after cycle testing indicates that the cathode is still intact, so our attention has been directed at XRD analysis for impurity phases in both the as-sintered and cycled cathode tapes.

Almost all of the tapes showed some evidence of oxygen loss, even though burnout and sintering of the tapes are normally done in flowing oxygen. When sintered above 1100°C, XRD indicates the presence of Li_2MnO_3. For tapes sintered at lower temperatures, Mn_3O_4 or Mn_2O_3 are generally detected; this low-temperature reduction may be due to burnout of the organic binder. In addition, the V_2O_5 sintering aid likely contributes a third phase to the system. If any of these phases coat either the $LiMn_2O_4$ grains or the cathode/electrolyte interface, they may have a profound influence on the cycling behavior of the cathode. Several tests are underway, where our thin-film deposition capability is being used to build thin-film batteries with layered cathodes, where a lower voltage and more resistive cathode is deposited over the $LiMn_2O_4$ spinel film. Although results are still preliminary, it is clear that a thin layer covering the spinel may lead to either a large difference between the charge and discharge voltages and/or a large difference between the observed charge and discharge capacities. Efforts are now being directed to achieving sintered tapes free of any second-phase contamination which may be interfering with the performance of the solid-state batteries.

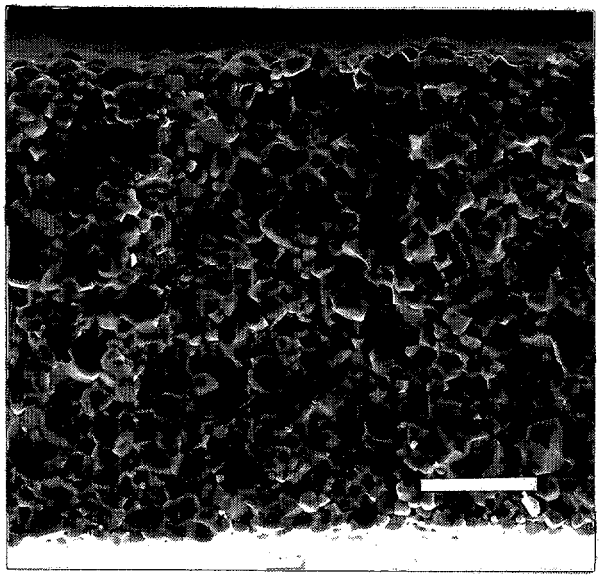

Figure 6. SEM fracture cross section of a $LiMn_2O_4$ tape sintered at 700°C. (Bar = 10 μm) The commercial $LiMn_2O_4$ powder was ball milled for 10 days and 4% V_2O_5 was added to the slip.

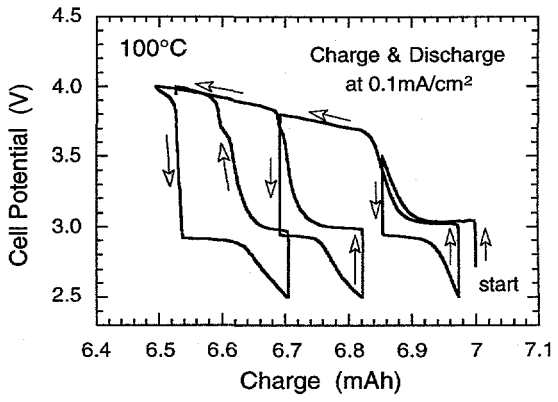

Figure 7. Initial charge/discharge steps of a hybrid battery at 100°C. The cathode is the same sintered tape as shown in Fig. 6; the estimated total Li capacity of this cathode corresponds to ~7 mAh.

ELECTRODES FOR AQUEOUS ELECTROCHEMICAL CELLS

Electrodes are being developed to identify low-cost metal hydrides for MH/NiOOH cells and improved metal oxides for electrochemical capacitors

Preparation of Improved, Low-Cost Metal Hydride Electrodes for Automotive Applications

James J. Reilly
Brookhaven National Laboratory, DAS-Bldg. 815, P.O. Box 5000, Upton NY 11973-5000
(516) 344-4502, fax: (516) 344-4071 ; e-mail: reilly@bnl.gov

Objectives

- Determine the properties and behavior of metal hydride electrodes with a view towards improving their lifetime, storage capacity and decreasing their costs.
- Determine structure of complex AB_5 electrode alloys.
- The creation of a realistic mathematical model of the behavior of the MH_x electrode.

Approach

- Determine thermodynamic properties of alloy hydrides used in electrodes.
- Fabricate and test hydride electrodes.
- Employ and develop X-ray absorption spectroscopy (XAS) methods to determine the electronic structure, the local atomic environment and corrosion of alloy hydride electrode materials.
- Employ neutron diffraction to determine crystal structure.

Accomplishments

- The crystal structure of $LaNi_{3.55}Co_{0.75}Mn_{0.4}Al_{0.3}$ was determined.
- The "Discrete Lattice Expansion" (DLE) hypothesis was tested.
- The addition of Zn to the KOH electrolyte inhibited corrosion in certain cases.
- Neutron diffraction was used to determine the expansion of $LaNi_{3.55}Co_{0.75}Mn_{0.4}Al_{0.3}$ from 10 to 300 K.
- A model for hydrogen transport in a two-phase solid system was developed.

Future Direction

- Reduce electrode costs by decreasing or eliminating Co in the electrode alloy.
- Systematically explore composition and function in AB_2 alloy electrodes.
- Determine the crystal structure of promising complex alloys.
- Improve performance of NiOOH cathode.

Crystal Structure of $LaNi_{3.55}Co0_{.75}Mn_{0.4}Al_{0.3}$. Two LaB_5 alloys were prepared. The composition of alloy 1 ($LaNi_{3.55}Co0_{.75}Mn_{0.33}Al_{0.3}$) was prepared using metals having the normal isotopic ratio. Alloy 2 of essentially the same composition was prepared using Ni isotopes in the ratio $^{58}Ni_{0.376}{}^{62}Ni_{0.623}$ so that the neutron scattering contributions of Ni would be zero while that of Co greatly increased. Neutron diffraction was carried out at the Hi Flux Beam Reactor at BNL and the neutron facility at the National Institute of Standards and Technology (NIST) in Gaithersburg, MD.

The diffraction patterns of alloys 1 and 2 were quite different and illustrated the effect of the null Ni sample on the peak intensities. Rietveld refinements of alloy 2 (null Ni) yielded the best agreement with the experimental data. In the final refinement the Mn and Al were all located on the 3g sites as the occupancies refined for the 2c sites were below the estimated standard deviations. The observed occupancies of Co of

0.23(1) and 0.52(1) for the 2c and 3g site, respectively, indicate a preference for the mid-plane 3g sites. However the actual distribution of Co is 31% on the 2c site and 69% on the 3g site. Substitution of the various subject metals for Ni does not change the $LaNi_5$ space group which remains P_6/mmm with a = 5.07136(8) Å, and c = 4.0546 Å.

Structure of $La(^{58}Ni_{0.376}{}^{62}Ni_{0.623})_{3.55}Co_{0.75}Mn_{0.33}Al_{0.3}D_{4.70}$. Alloy 2, charged with deuterium, was also examined using the high-resolution neutron powder diffractometer BT1 at NIST. The site preference of Co to occupy the 3g over the 2c sites was confirmed. Again Al and Mn were determined to occupy the 3g sites exclusively. Four of the possible five deuterium sites were found to be occupied in the following order : the 12n site with n D atoms = 2.28(3) (D(3)), the 6m site with n = 1.70(3) (D(2)), the 12o site with n = 0.55(2) (D(1)) and the 4h site with n = 0.17(1) (D(4)). The space group remains P6/mmm with a = 5.36399(7) Å and c= 4.2704(2) Å.

Coefficient of thermal expansion. The coefficients of thermal expansion of $LaNi_{3.55}Co_{0.75}Mn_{0.33}Al_{0.3}$ and its deuteride, $LaNi_{3.55}Co_{0.75}Mn_{0.33}Al_{0.3}D_{5.8}$, were determined using neutron diffraction. The crystal symmetry remained hexagonal from 10 to 300 K. The expansion of the a axis for both the metal and the deuteride phases are 0.2 and 0.3%, respectively, over the temperature range cited. However, the c-axis expansion in the deuterided sample is only 1/6 that of the c axis of the metal lattice. Obviously the insertion of deuterium greatly stiffens the lattice in the c direction.

Discrete Lattice Expansion (DLE). An important parameter in the corrosion of MH electrodes is the degree of alloy expansion (*i.e.*, DLE) due to the uptake of hydrogen. DLE is defined as the expansion taking place upon the conversion of the α phase to the β phase. It is hypothesized that an alloy which has a relatively short plateau (or miscibility gap in the H-metal phase diagram) in the pressure-composition isotherm would corrode at a lower rate than a similar alloy with a wide plateau. This theory was tested using the relatively simple AB_5 alloy $LaNi_{4.7}Al_{0.3}$.

In Fig. 8, X-ray diffraction patterns are illustrated for as-received and ball-milled (1.25 h) crystalline $LaNi_{4.7}Al_{0.3}$. Pressure-composition isotherms were obtained. The isotherms for crystalline $LaNi_{4.7}Al_{0.3}$ had wide, flat plateaus whereas those of ball-milled material had sloping plateaus. DLE was substantially less for the ball-milled alloys.

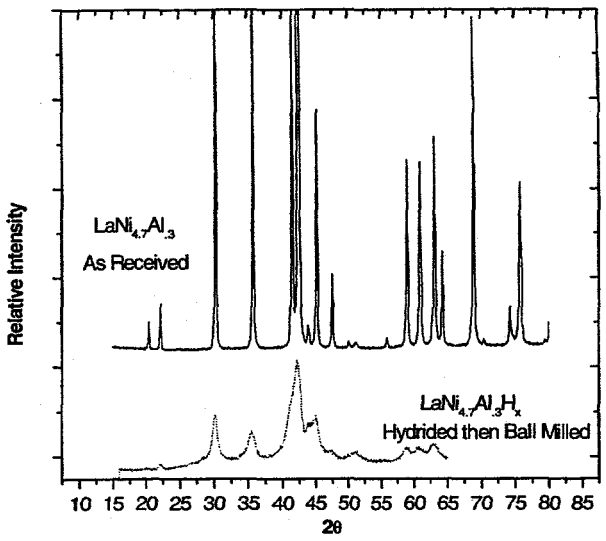

Figure 8. X-ray diffraction patterns of $LaNi_{4.7}Al_{0.3}$.

The cycle lives of electrodes from ball-milled $LaNi_{4.7}Al_{0.3}$ were greatly increased over those made from crystalline material although their initial capacities were much reduced. The ball-milled sample was annealed for about 0.5 h at 500°C to regain alloy crystallinity. The cycle life of an electrode incorporating recrystallized $LaNi_{4.7}Al_{0.3}$ was greatly reduced compared to that of the ball-milled alloy even though its initial capacity was the same. The results of the investigation support the validity of the DLE hypothesis.

Effect of Zn on corrosion of AB_5 electrodes. In collaboration with S. Srinivasan and co-workers (Texas A&M University), we studied the effect of Zn ions on the corrosion of several types of AB_5 (B_5 = $Ni_{3.55}Co_{0.75}Mn_{0.4}Al_{0.3}$) alloy electrodes by XANES of Ni.

Four different alloy compositions were evaluated; LaB_5, $La_{0.8}Ce_{0.2}B_5$, MmB_5 and Ce free MmB_5 (Mm^*B_5) (Mm = mischmetal) which were prepared by arc melting under a He atmosphere and then annealed under He for 72 h. XRD analyses showed that the samples were single-phase alloys with a hexagonal $CaCu_5$ structure. The electrodes for cycle-life measurements were prepared after gas phase pre-activation. All electrochemical cycling experiments were conducted in a flooded, vented cell with 6 M KOH. The charge/discharge rate was C/5, the cut-off voltage on charge was -1.2 V and for discharge was -0.7 V *vs.* Hg/HgO reference. The concentration of Zn in the 6 M KOH electrolyte

was varied between 0.1-1 M. The measurements were carried out on cycled electrodes under *ex situ* conditions using beam line X11A at the National Synchrotron Light Source (NSLS).

The percent expansion of the various alloys plays a significant role in determining cycle life. Cycling the samples with 0.5 M ZnO in the electrolyte (higher concentrations up to 1 M ZnO had no further change) had a major effect for samples without Ce substitution. The cycle lives of Ce-free samples (LaB_5 and Ce-free Mischmetal) increased by about 45%. The Ce-containing samples remained unaffected.

XANES results at the Ni K edge indicated the following: 1) Corrosion is directly proportional to the buildup of $Ni(OH)_2$ in the surface region of the alloy particles. 2) The presence of Zn in the electrolyte inhibited the buildup of $Ni(OH)_2$ on the surface of Ce-free electrodes. 3) Cerium also inhibits the formation of $Ni(OH)_2$ thus the presence of Zn had little effect with Ce-containing electrodes. Therefore, it was concluded that zincate ions in 6 M KOH electrolyte impart surface protection in alloys where such passive protection does not already exist. The exact mechanism by which zincate ions provide this protection will be the subject of future work.

Hydrogen Transport in Solids. A model of steady-state H atom transport in a metal-metal hydride foil electrode of uniform thickness was completed which uses a phenomenological transport equation that incorporates the gradient of the chemical potential of hydrogen deduced from the operative pressure-composition isotherm. The model illustrates that the activity coefficients of H in the system are not constant and, consequently, the Fickian diffusion equation must be modified accordingly.

PUBLICATIONS

G.D. Adzic, J.R. Johnson, S. Mukerjee, J. McBreen and J.J. Reilly, "Function of Cobalt in AB_5H_x Electrodes," *J. of Alloys and Compounds*, **253-254**, pp 579-582 (1997).

G.D. Adzic, J.R. Johnson, S. Mukerjee, J. McBreen and J.J. Reilly, "Corrosion 0f AB_5 Metal Hydride Electrodes," *Proc. of the Symposium on Electrochemical Surface Science of H Adsorption and Absorption into Metals, Alloys and Intermetallics*, G Jerkiewicz, A.R. Landgrebe and P. Marcus, eds., Vol. 97-16, pp 288-300, The Electrochemical Soc., Pennington NJ, 1997.

S. Mukerjee, J. McBreen, J.R. Johnson, G. Adzic, J.J. Reilly, M.R. Marrero, M.P. Soriaga, M.S. Alexander, A. Visintin and S. Srinivasan, "Effect of Zn Additives to the Electrolyte on the Corrosion and Cycle Life of Some AB_5H_x Electrodes," *J. Electrochem. Soc.* **144**, L258, (1997).

S.W. Feldberg and J.J. Reilly, "Phenomenological Treatment of Hydrogen Transport in a Metal/Metal Hydride System," *J. Electrochem. Soc.* **144** , 4260 (1997).

Optimization of Metal Hydride Properties in MH/NiOOH Cells for Electric Vehicle Applications

Ralph E. White
Department of Chemical Engineering, University of South Carolina, Columbia, SC 29208
(803) 777-7314; fax: 803)777-8265; e-mail: rew@sun.che.sc.edu

Objectives

- Optimize the alloy composition of metal hydride electrodes by microencapsulation of hydrogen-storage alloys.
- Develop a theoretical model to evaluate the equilibrium potential and the exchange current density as a function of state of charge of the electrode.
- Develop improved metal hydride electrodes for MH/NiOOH batteries.

Approach

- Prepare bare and Co-coated $LaNi_{4.27}Sn_{0.24}$ electrodes for determination of transport and electrochemical kinetic parameters.
- Determine the cycle lives of bare and electroless coated alloys.
- Develop a mathematical model for evaluation of exchange current density and other electrochemical kinetic parameters for porous electrodes.

Accomplishments

- The three-step process for electroless plating of Ni, Ni-P, Co and Co-P has been simplified to a one-step process thereby eliminating the costly activation step with palladium and tin chloride.
- $LaNi_{4.27}Sn_{0.24}$ electrodes were characterized using electrochemical techniques at different alloy weights and binder contents.
- Microencapsulation of the hydrogen storage alloys with electroless Co was found to improve the performance of the negative electrode. Cobalt has several advantages over other electroless coatings for microencapsulation of metal hydrides. The miroencapsulation resulted in an adherent magnetic deposit. Also, the discharge curves indicated an additional faradaic contribution to the capacity.
- A theoretical model for predicting the thermodynamic and kinetic parameters of the hydride electrode has been developed.

Future Directions

- Optimize the cycle lives of $LaNi_{4.27}Sn_{0.24}$ alloys by decreasing the pulverization rate and by microencapsulation.
- Develop a mathematical model to predict the deterioration behavior of M-H and optimize the particle size of the electrode.

An analytical model for the discharge of the metal hydride electrode under galvanostatic conditions was developed. The discharge model and the differential equations derived are general in nature and can be used for any hydride material. The analytical model coupled with the Margules thermodynamic correction for the activity coefficients was used to study the electrode under various conditions.

The effects of the particles size on the power density and energy density of the metal hydride electrode were determined. At low current densities, the energy density approaches a theoretical limit, which is a function of the open circuit potential. The energy density increases slightly with a decrease in the particle size. However, a more pronounced effect is seen on the power density of the alloy. A smaller particle reduces the time required for hydrogen to reach the surface. This significantly increases the power density . However, reducing the particle size also results in exposing more area of the active materials to the electrolyte. Microencapsulation of small particles decreases dramatically the corrosion rate.

Microencapsulation of particles with a thin coating on the surface has been found to improve the performance of metal hydride alloys. However, carrying this out on a large scale is limited by the number of steps involved in the electroless plating process. The multi-step process for electroless plating of Co, Co-P, Ni, Ni-P and Co-Ni-P alloys has been simplified to a one-step technique. Conventional electroless plating of powders involves a number of steps including the costly pretreatment and activation steps with tin chloride and palladium chloride. Eliminating these steps and simplifying the microencapsulation process would make it economically feasible for practical battery applications.

Experimental results showed that a Co coating significantly increases the electrode discharge capacity. The electrochemical impedance spectroscopy technique was used to determine various resistive components in the electrodes and electrolyte by fitting an equivalent circuit to the experimental data.

PUBLICATION

B.N. Popov, G. Zheng and R.E. White, "Effect of Temperature on Performance of M-H Electrode," *J. Appl. Electrochem.* **27,** 1328 (1997).

Microstructural Modeling of Highly Porous MH/NiOOH Battery Substrates

Ann Marie Sastry
Department of Mechanical Engineering and Applied Mechanics, The University of Michigan, Ann Arbor, MI 48109-2125
(313) 764-3061; fax: (313) 747-3170; e-mail: amsastry@engin.umich.edu

Objectives

- Develop predictive capability for performance of Li-ion negative substrates, comprised of fibrous and particulate carbon, using combined stochastic-mechanical simulation. Validate modeling effort with mechanical, transport and electrochemical testing of cells.
- Develop predictive capability for performance of Ni/MH positive substrates, comprised of fibrous and particulate Ni, and fibrous Ni, using combined stochastic-mechanical simulation.

Approach

- Develop stochastic geometry models for key morphologies of Li-ion electrode materials, including whiskers (~1 μm), fibers (~10 μm) and spherical particles (<10 μm) based on carbonaceous materials.
- Assess the degradation in physical properties of electrode materials under likely cell cycling loads, especially electrical conductivity, correlating the degradation processes with cell operation by *post-mortem* analyses of the electrode microstructure.
- Extend mechanics solutions to model the load transfer between fibrous and particulate materials, and thus to optimize the ratios of each in Li-ion cells.

Accomplishments

- Novel stochastic network generation technique developed, with sufficient simulations performed to model the effects of manufacturing parameters upon important descriptors of connectivity.
- Validated novel technique for calculation of transport coefficient (electrical resistivity) using the stochastic approach and for determination of mechanical response of fibrous networks
- Development of techniques for coupled transport/mechanics initiated.

Future Direction

- Continue large-scale simulation of mechanical damage and transport behavior in random networks of electrode materials for Li-ion cells.

The objective of this program is to develop predictive capability for performance of two key types of automotive cells: Li-ion and Ni/MH. Degradation of battery electrode materials is currently a persistent problem during charge/discharge cycling of both of these advanced battery systems.

Several types of Ni/MH substrate materials have now been completely characterized, for transport, mechanical and electrochemical performance. Experiments have been completed on both cycled and uncycled materials, and the central hypothesis of this study has now been validated: that mechanical and transport properties in cycled substrates are measurably and predictably reduced via material connectivity loss. The statistical techniques used to predict the connectivity of the material microstructures have been used to identify broad categories of superior microstructures for use in batteries. Figure 9 illustrates the simulations performed and their application to materials design: the material connectivity, described as

number of bonds per unit cell, is calculated for networks of a given standard deviation in material orientation, for a family of curves corresponding to approximate fiber volume fraction. These types of simulation allow prediction of both material variability and material performance, using physically realistic network parameters.

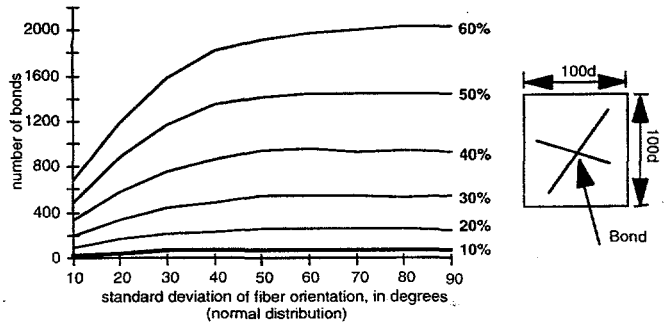

Figure 9. Material connectivity *vs.* orientation, for a number of fiber volume fractions.

Mechanical properties and damage progression in these materials has also been determined via simulation of loads applied to these stochastic networks. Figure 10 illustrates these, showing material modulus versus fiber volume fraction for a number of fiber aspect ratios.

Damage simulations have addressed key questions concerning the micromechanisms of failure in the substrate materials. Work in Li-ion is focused on the effect of particulate fraction in these materials. A graphite negative electrode in Li-ion cells undergoes an expansion in the basal plane of about 10% when Li intercalation reaches a capacity of 372 mAh/g (equivalent to LiC_6). During charge/discharge cycling, the graphite structure undergoes expansion and contraction as Li ions are intercalated/deintercalated, much as the positive plate in a Ni/MH cell swells. The mechanical stress and physical changes that occur play a role in the cycle life of graphite electrodes in Li-ion cells. The nature of the stresses will be explored through similar simulation and experimental validation.

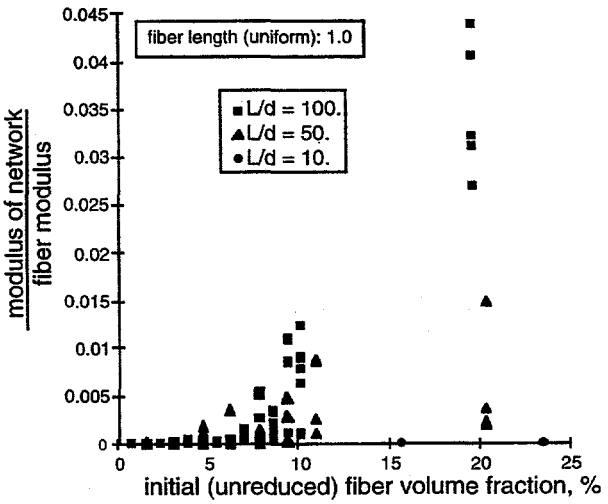

Figure 10. Network modulus *vs.* volume fraction, for varying fiber aspect ratio.

PUBLICATIONS

A.M. Sastry, X. Cheng and C.W. Wang, "Mechanics of Stochastic Fibrous Networks," *J. Thermoplastic Composite Materials*, (1997), in press.

A.M. Sastry, X. Cheng and S.B. Choi, "Transport in Fibrous Battery Electrode Substrates," *Proc. of the 1997 International Mechanical Engineering Congress & Exposition*,, **MD80**: 331-338, Dallas, TX, November 16-21, 1997.

A.M. Sastry, S.B. Choi and X. Cheng, "Damage in Composite NiMH Positive Electrodes," *Proc. of the 1997 International Mechanical Engineering Congress & Exposition*, **MD80**: 251-258, Dallas, TX, November 16-21, 1997.

A.M. Sastry, X. Cheng and C.W. Wang, "Mechanics of Stochastic Fibrous Networks," *Proc. of the 12th Annual Technical Conference of the American Society for Composites*, 1167-1173, Dearborn, MI, October 6-8, 1997.

Sol-Gel Derived Metal Oxides for Electrochemical Capacitors

Marc A. Anderson
Water Chemistry Program, University of Wisconsin-Madison, 660 North Park Street, Madison, WI 53706
(608) 262-2470; fax: (608) 262-0454; e-mail: marc@engr.wisc.edu

Objectives

- Investigate the chemical and materials properties of the NiO/Ni system for electrochemical capacitors.
- Model and design metal oxide electrodes for improved electrochemical capacitors.

Approach

- Utilize sol-gel processing techniques to fabricate thin-film electrodes for electrochemical capacitors.

Accomplishments

- Observed that NiO is a viable electrode material for capacitors when cycled at potentials less than 300 mV *vs.* saturated calomel electrode (SCE).

Future Direction

- Project has been completed.

The objective of this research is to investigate the chemical and materials properties of the NiO/Ni system for electrochemical capacitors (ultracapacitors), including exploratory research on sol-gel processing methods to fabricate thin-film ultracapacitors.

Microporous thin films of sol-gel-derived, non-stoichiometric NiO on vapor-deposited thin-film gold electrodes have been characterized to determine optimal operating potentials and to investigate their primary charge storage mechanism. Cyclic voltammetry, chrono-potentiometry, and impedance spectroscopy have demonstrated that the behavior of a newly prepared NiO electrode is very close to that of an ideal ultracapacitor material. Cycling these electrodes at potentials no higher than 300 mV vs. the SCE preserves this ultracapacitor-like behavior for up to at least several hundred cycles. Charge transfer in this potential domain is due to a surface reaction that, among nickel compounds, is unique to non-stoichiometric NiO. It is now believed that charge storage in these devices primarily proceeds by means of a surface redox reaction involving the partial oxidation of Ni^{2+} (NiO) by proton transfer. The high surface area of these electrodes supports a surface reaction with a charge capacity in excess of 100 times that of a theoretical flat NiO surface of the same geometric area. These materials have shown specific capacitances as high as 260 F/g in 1 M LiOH.

When cycled at potentials less than 300 mV, NiO is a viable novel material for use in ultracapacitors. However, if a NiO electrode is cycled at potentials higher than 300 mV, the bulk of the electrode is gradually activated, and the electrochemical behavior of the film becomes very similar to that of electrochemically precipitated $Ni(OH)_2$. Charge transfer in $Ni(OH)_2$ electrodes occurs in the bulk and is less useful for application in ultracapacitors. However, NiO cannot be transformed into $Ni(OH)_2$. Rather, it is believed that such changes may be due to increases in the non-stoichiometry of the bulk of the electrode, transforming the previously inactive bulk into the electrochemically active non-stoichiometric form. It is most important to note that, in order to utilize these materials in electrochemical capacitors, activation of the bulk should be avoided. Therefore, it is critical to understand the surface reactions that occur in this system.

PUBLICATIONS

K.-C. Liu and M.A. Anderson, "Getting a Charge Out of Microporous Oxides: Building a Better Capacitor," *Mat. Res. Soc. Symp. Proc.* **432**, 221-229, 1997.

K.-C. Liu and M.A. Anderson, "Performance of UW-Thin Cap Ultracapacitors," in *Electrochemical Capacitors II*, F.M. Delnick, D. Ingersoll, X. Andrieu and K. Naoi, eds., **PV-96-25**, p. 85, The Electrochemical Society, Pennington, NJ, 1997.

K.-C. Liu and M.A. Anderson, "The Effect of Electrolytes on Nickel Oxide Based Electrochemical Capacitors," in *Electrochemical Capacitors II*, F.M. Delnick, D. Ingersoll, X. Andrieu and K. Naoi, eds., **PV 96-25**, p. 97, The Electrochemical Society, Pennington, NJ, 1997.

COMPONENTS FOR NONAQUEOUS CELLS

Metal/electrolyte combinations that improve the rechargeability of nonaqueous cells are under investigation.

Novel Lithium/Polymer-Electrolyte Cells

Elton J. Cairns and Frank R. McLarnon
90-1142 , Lawrence Berkeley National Laboratory, Berkeley CA 94720
(510) 486-4636; fax: (510) 486-4260; e-mail: ejcairns@lbl.gov / frmclarnon@lbl.gov

Objectives

- Investigate the behavior of electrodes in high-performance rechargeable batteries, and investigate means for improving their lifetime and performance.
- Improve the utilization of the sulfur electrode.
- Identify new electrode structures which will eliminate or minimize fundamental mechanisms of capacity loss of Li/MnO_2 cells.

Approach

- Fabricate and test Li/polymer electrolyte/sulfur cells.
- Use a completely new approach to synthesize a homogeneous "nano-scale" dispersion of a MnO_x entity inside a polymer matrix.

Accomplishments

- Greatly improved utilization (in the range of 80-90%) of the active material for the reaction $2\ Li + S \rightarrow Li_2S$ was obtained, corresponding to capacities of 1350-1500 mAh/g sulfur.
- Novel aerogel $Li_xMn_yO_4$ powders with very high surface area were prepared using a sol-gel technique and supercritical drying with CO_2.

Future Directions

- Use *in situ* UV/VIS spectroscopy to investigate the mechanism by which the sulfur electrode operates.
- Optimize the performance of MnO_x including post-test characterization to identify the structure of the active component.

Li/S Cells. Previously, galvanostatic cycling of early Li/polymer/S cells yielded poor active material utilization. In addition, unusual phenomena were observed, including discoloration of the polymer electrolyte surrounding the sulfur electrode and very long charge half-cycles with flat voltage plateaus. To address the cause(s) of these phenomena, different polymer and polymer gel electrolytes were tested, including amorphous polyethylene oxide. However, these changes did not significantly alter the cell characteristics stated above.

Following the issuance of a U.S. patent to PolyPlus Battery Company, Berkeley, CA, for Li/polymer/S batteries, modifications were made to the composition and processing of electrodes and electrolyte in an effort to duplicate the high-capacity cell cycling claimed in this patent.

Following a typical protocol, in which a salt-free polyethylene oxide-based "electrolyte" is described, a sulfur electrode was produced with much less Li salt than previously used. In addition, dispersant was excluded from the electrode, and the electrodes were processed by casting directly onto the current collector, yielding thinner electrodes. We also used a more highly structured, lower-density acetylene black which yielded better dispersions. These changes, as well as improvements to the cell design, including accommodation of a reference electrode, have resulted in greatly improved utilization (in the range of 80-90%) of the active material for the reaction $2\ Li + S \rightarrow Li_2S$, corresponding to capacities of 1350-1500 mAh/g sulfur. This amounts to about 750 mAh/g positive electrode (containing 50 wt% S). More than 20 cycles at capacities above 320 mAh/g S have been achieved, but longer cycle lives are desired. The electrolyte discoloration persists, and is probably caused by the solubility of some sulfur-containing species in the electrolyte. This is being investigated using *in situ* UV-VIS spectroscopy in specially-designed spectroelectrochemical cells. The design of these cells is particularly challenging because of the need for a relatively unobstructed optical path through a functioning Li/S cell. The most-recent design is showing promise, and we anticipate gathering spectra of good quality in the near future. These spectra will provide a rather detailed understanding of how the sulfur electrode is functioning, which will provide guidance for further improvements in cell performance and lifetime.

Li/MnO_2 Cells. Novel aerogel $Li_xMn_yO_4$ powders with very high surface area have been prepared using a sol-gel technique and supercritical drying with CO_2. Preliminary cell tests with this material showed good performance with capacities of 175 mAh/g, but significant capacity fading during cycling. The cause of this behavior was traced to the composition of the aerogel. Improved synthesis methods have been employed recently, making use of ion-exchange techniques for introducing the correct amount of Li to the material. These materials were characterized by XRD to verify amorphous structure, thermogravimetric analysis (TGA) to determine dryness and thermal stability, and SEM to measure the micropore size (10 nm). The newly synthesized material will be used to produce cells for performance and cycle-life evaluation.

PUBLICATIONS

E.J. Cairns, "Overview of the Current Status and Problems for Rechargeable Batteries," *Progress in Batteries & Battery Materials* **16,** 237, (1997).

K.A. Striebel, S.J. Wen, D.I. Ghantous, and E.J. Cairns, "Novel Nanodisperse Composite Cathode for Rechargeable Lithium/Polymer Batteries," *J. Electrochem. Soc.* **144,** 1680 (1997).

New Cathode Materials

M. Stanley Whittingham
Chemistry and Materials Research Center, State University of New York at Binghamton, Binghamton, NY 13902–6000
(607) 777-4623; fax: (607) 777-4623; e-mail: stanwhit@binghamton.edu

Objectives

- Synthesize and evaluate oxides of transition metals for alkali-metal intercalation electrodes.
- Identify new intercalation compounds for positive electrodes in advanced nonaqueous secondary batteries.

Approach

- Synthesize metal oxides that have crystallographic structure to permit facile intercalation of Li ions.
- Characterize the metal oxide structures by XRD analysis and evaluate materials in electrochemical cells.

Accomplishments

- Cycling studies of $Li_xM_yMnO_2$ (M = Li, Na, K, Rb, Mg, Ba) and on the spinel $LiMn_2O_4$ showed that the highest capacity after several cycles was obtained when M = K, which provided an intermediate interlayer spacing, and has the most crystalline lattice.
- Determined range of structures formed by vanadium oxides, and identified some that may be good models for manganese oxides.

Future Directions

- Continue synthesis and electrochemical studies of manganese oxides.

The objective of this project is to synthesize and evaluate first-row transition metal oxides for Li-intercalation electrodes in advanced nonaqueous rechargeable batteries. Mild hydrothermal techniques are being used for the synthesis, and where this technique does not lead to the highest oxidation states, methods will be explored to drive the transition metal to its highest oxidation state. Manganese oxides are particularly attractive as the cathode, and means of stabilizing the layered manganese dioxide structure are being explored.

The synthesis of layered manganese compounds by the mild hydrothermal aqueous decomposition reaction of alkali permanganate at 170°C was extended to include rubidium, magnesium and barium to determine the optimum interlayer cation. Our prior results indicated that the larger the cation the better the cycling, *i.e.*, K>Na>Li. The structure of the alkali manganese oxide is the same as that of $LiCoO_2$ and related to $LiTiS_2$. The rubidium compound had inferior crystallinity, and converted to hollandite-type $Rb_2Mn_8O_{16}$ on heating up to 800°C in air. The magnesium and barium manganates were essentially amorphous to X-rays like a sol-gel.

Reaction of K_yMnO_2 with n-butyl Li showed an uptake of 1.0 Li/Mn, and the electrochemical behavior of all these compounds shows a continuous curve indicative of a single phase, $Li_xM_yMnO_2$, similar to that observed in the layered disulfides. Moreover, most of the capacity is between 3.5 and 2.5 V, a practical voltage range. The Mg compound had an initial cell voltage of 3.7 V and capacity of 195 mAh/g, significantly higher than the Ba compound. The data for the 1st and 6th cycles are shown in Table 3, and indicate that the potassium compound still has the best performance, >460 Wh/kg. This is essentially the same as those of $LiCoO_2$ and $LiTiS_2$.

The spinel $LiMn_2O_4$ is being investigated as a possible replacement for $LiCoO_2$; however it only cycles 0.5 Li/Mn. To ascertain the comparable data for the spinel $LiMn_2O_4$, samples of the spinel were formed and cycled in the same electrolyte in three potential regimes: 1.9-3.1, 1.9-3.9 and 1.9-4.1 V. The capacity retention is not significantly increased by raising the charge voltage from 3.9 to 4.1 V. In all cases the capacity falls rapidly as the cell is cycled, just as in the layered Li_xMnO_2.

Table 3. Cell capacity of M_yMnO_2 cathodes compared with the spinel $LiMn_2O_4$.

Capacity →	1st Cycle	1st Cycle	6th Cycle
M in M_yMnO_2	Li/Mn	mAh/g	mAh/g
Li	0.58	172	74
Na	0.56	158	124
K	0.60	166	144
Rb	0.47	121	55
Mg		195	*140
Ba		75	
Spinel (3 volt)	0.40	119	74

*2nd cycle

The spinel $LiMn_2O_4$ is being investigated as a possible replacement for $LiCoO_2$; however it only cycles 0.5 Li/Mn. To ascertain the comparable data for the spinel $LiMn_2O_4$, samples of the spinel were formed and cycled in the same electrolyte in three potential regimes: 1.9-3.1, 1.9-3.9 and 1.9-4.1 V. The capacity retention is not significantly increased by raising the charge voltage from 3.9 to 4.1 V. In all cases the capacity falls rapidly as the cell is cycled, just as for the layered Li_xMnO_2.

The rapid degradation of capacity on cycling of the layered Li_xMnO_2 and spinel is almost certainly due to diffusion of manganese from the MnO_2 layers, as the optimum arrangement of the Mn and Li ions is almost certainly a function of the Li content. Figure 11 shows the cell voltage for the layered and cubic spinel forms of lithium manganese oxide. It clearly indicates that at high

Li values, x>0.5 in Li_xMnO_2 or $Li_{2x}Mn_2O_4$, the layered phase is more stable whereas at lower Li contents the cubic spinel phase is more stable. Thus, during cycling there will be a tendency for each to interconvert during the cycling process.

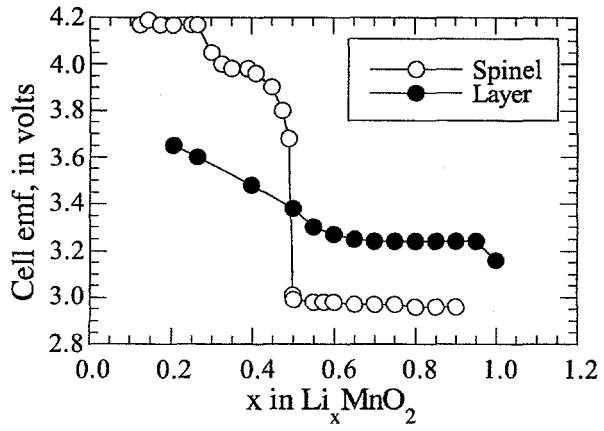

Figure 11. Cell voltages of the layered and spinel phases of manganese oxide (Bruce and Whittingham).

The better results observed with potassium leads us to conclude that if the layer structure can be stabilized to prevent Mn migration into the interlammellar region, then the capacity might be maintained during extended cycling. Two approaches are being used, stabilization using partial substitution of Ni for Mn, and the use of pillaring ions (*e.g.*, potassium).

An attempt to incorporate Ni, in place of an alkali ion, into layered manganese dioxide by the hydrothermal decomposition of tetramethyl ammonium (TMA)•MnO_4 in the presence of Ni salts led to the formation of a totally new structure with the formula $NiMnO_3$ rather than a simple layered manganate Ni_yMnO_2. A collaboration with John Greedan of McMaster University confirmed that the compound contains predominantly Ni^{3+} and Mn^{3+}, a very unusual combination (Fig. 12). This compound reacts with n-butyl lithium to give $LiNiMnO_3$ with minimal structural change, but reaction in an electrochemical cell is very slow.

While exploring the zinc-vanadium-oxygen phase we discovered the new compound $Zn_3(OH)_2V_2O_7•2H_2O$, which has the very interesting structure shown in Fig. 12. The sheets consist of zinc oxyhydroxide sheets held apart by -V-O-V- pillars akin to the -Al-O-Al- pillars in β-alumina. The water molecules (open circles in figure) are readily removed upon heating with structure retention. Lithium ions are readily intercalated, and we are now attempting to form an analogous manganese compound, which we will attempt to oxidize to remove the hydrogen atoms, *i.e.*, convert hydroxide to oxide.

Summary of Vanadium Oxide Compounds. We have systematically studied the hydrothermal formation of vanadium oxides, from a 1:2:1 reaction mixture of V_2O_5 powder, TMA aqueous solution and LiOH. The product formed was found to be a strong function of the initial pH of the reaction medium. We have characterized the $TMAV_8O_{20}$ phase, and shown it to be electrochemically active. The sol-gel like material formed under the most acidic conditions is more crystalline than previously reported xerogels and may allow us to determine the structure of that material. The $TMAV_3O_7$ was very readily oxidized to $TMAV_3O_8$, and as expected, showed a five-fold improved electrochemical capacity, confirming the critical need to attain the highest oxidation state possible.

We also studied the effect of replacing the Li ions with Zn and Fe. Several new layered compounds were formed, including the double-sheet $Zn_yV_2O_5$ and $TMA_{0.15}Fe_{0.1}V_2O_5$. Their electrochemical behavior suggests that double-sheet structures, such as xerogels, are more structurally stable and cycle well in Li cells. This study also resulted in the discovery of the pillar compound, $Zn_3(OH)_2V_2O_7•2H_2O$, discussed above that might be a good model for a desired manganese oxide cathode.

PUBLICATIONS

T.A. Chirayil, P.Y. Zavalij and M.S. Whittingham, "$N(CH_3)_4V_3O_7$: Critical Role of pH in Hydrothermal Synthesis of Vanadium Oxides," *Chem Commun.* **33** (1997).

R. Chen and M.S. Whittingham, "Cathodic Behavior of Alkali Manganese Oxides from Permanganate," *J Electrochem Soc.* **144**, L64 (1997).

M.S. Whittingham, R. Chen, T. Chirayil and P. Zavalij, "The Intercalation and Hydrothermal Chemistry of Solid Electrodes," *Solid State Ionics* **94**, 227 (1997).

F. Zhang, P.Y. Zavalij and M.S. Whittingham, "Hydrothermal Synthesis of Iron and Zinc Double Vanadium Oxides Using the Tetramethyl Ammonium Ion," *Mater. Res. Bull.* **32**, 701 (1997).

T. Chirayil, P.Y. Zavalij and M.S. Whittingham, "Hydrothermal Synthesis of Vanadium Oxides," *Mater. Res. Soc. Proc.* **453**, 135 (1997).

M.S. Whittingham, E. Boylan, R. Chen, T.G. Chirayil, F. Zhang and P.Y. Zavalij, "Hydrothermal Synthesis of Novel Vanadium Oxides," *Mater. Res. Soc. Proc.***453**, 115 (1997).

R. Chen, P.Y. Zavalij and M.S. Whittingham, "New Manganese Oxides by Hydrothermal Reaction of Permanganates," *Mater. Res. Soc. Proc.* **453**, 653 (1997).

T. Chirayil, P.Y. Zavalij and M.S. Whittingham, "Synthesis and Characterization of a New Vanadium Oxide, $TMAV_8O_{20}$," *J. Mater. Chem.* **7**, 2193 (1997).

M.S. Whittingham, "The Relationship Between Structure and Cell Properties of the Cathode for Lithium Batteries, " in *Lithium Batteries*, O. Yamamoto and M. Wakihara, eds. 1997, Kodansha: Tokyo.

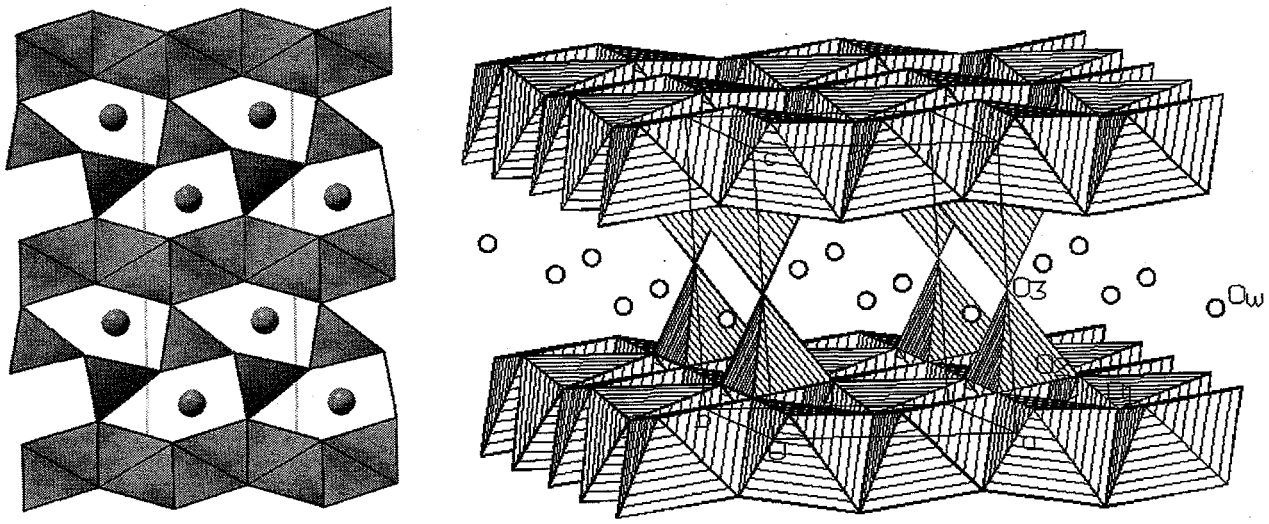

Figure 12. Structures of (left) $NiMnO_3$ and (right) $Zn_3(OH)_2V_2O_7 \cdot 2H_2O$.

Solid Electrolytes

Lutgard C. De Jonghe
62-203, Lawrence Berkeley National Laboratory, Berkeley CA 94720
(510) 486-6138; fax: (510) 486-4881; e-mail: lcdejonghe@lbl.gov

Objectives

- Fabricate and study novel composite electrolytes which combine the advantages of a protective thin-film single-ion conductor with a conventional elastomeric polymer electrolyte for EV applications.
- Develop a suitable composite electrolyte material for use in alkali metal/polymer cells.

Approach

- Synthesize and characterize a Li single-ion conductor combined in a single composite membrane acting as a separator in rechargeable Li batteries.
- Employ AC and DC techniques (e.g., galvanostatic charging and discharging, four-probe techniques, impedance spectroscopy and pulse testing) and thermal measurements to characterize solid-state batteries, as well as the properties of the individual components and interfaces.

Accomplishments

- Conductivities as high as 10^{-6} S/cm at 80°C were obtained with two-phase nanocomposite mixtures with no added salt or plasticizers, values which are comparable to or greater than those of recently developed dry single-ion conducting polymers.

Future Directions

- Continue work on nanocomposites.
- Expand the theory and develop methods for measuring transport properties in multi-component systems (*e.g.*, gels and composites).

The goals of the present research program are to fabricate and study novel composite electrolytes which combine the advantages of a single-ion conductor with a conventional elastomeric polymer electrolyte. Synthesis of smectic clay-polyethylene oxide (PEO) nanocomposites is also underway. Prior to use in electrochemical systems, the clay must be purified, ion-exchanged (Li for Na) and dried to remove water. It is then suspended in acetonitrile and PEO is added. At a weight ratio of ~0.3 g PEO per g of clay, nanocomposites self-assemble. The product may then be filtered and dried.

X-ray diffraction was used to determine the inter-layer spacings; 001 d-spacings for the synthesized nanocomposites become larger as polymer content increases, until a limiting value is reached. The maximum polymer uptake for polymers with average molecular weights above 1000 (PEO and amorphous PEOs) is about 0.7 g/g laponite, and the largest d-spacing ranges from about 18-21 Å. For polyethylene glycol dimethyl ether (PEGDME)-1000, the maximum uptake seems to occur at about the same composition, but the d-spacing expands to nearly 23 Å. An even larger maximum d-spacing and polymer uptake occurs when PEGDME-500 is used: about 24 Å and over 1g/g laponite. Differential scanning calorimetry (DSC) results indicate that the maximum polymer uptake is a function of the average molecular weight; slightly less than 0.7g/g is intercalated for polymers above MW=1000, slightly more than this is intercalated for PEGDME-1000, and about 1.1 g/g is intercalated for PEGDME-500. Thus, samples containing more than these amounts of polymers are true composites rather than nanocomposites, *e.g.*, polymer is located outside the particles as well as within the galleries.

Thermogravimetric analyses of laponite and representative polymer-laponite nanocomposites and composites were performed. PEO and amorphous PEOs generally begin to decompose at about 300-350°C, and are completely burned away by 400°C (under nitrogen, 10°C/min). Nanocomposites and composites show similar behavior, indicating that the thermal stability is similar to that of typical ion-conducting polymers under consideration for battery applications. Weight loss below this temperature can be attributed to water evaporation. An air-dried laponite film contains about 16% water, most of which is lost below 100°C, or within the first few minutes of heating. It is apparent that the polymer-containing films, which were not subjected to heat or vacuum before TGA analysis, contain markedly less water. This indicates that the water located between the silicate sheets is readily replaced by polymer in the nanocomposites and composites, although the substitution is incomplete for small amounts of polymer. Like laponite, the nanocomposites are easily dried under vacuum or during heating, but they rapidly rehydrate upon exposure to the atmosphere. Polymer compositions calculated from the weight loss above 300°C in the TGA traces were identical to the expected values, within experimental error.

Conductivities for representative nanocomposites, composites and salt-containing composites, containing PEO or amorphous PEOs were obtained as a function of temperature. Note that, except for materials containing salts, the reported values are single-ion conductivities for materials without added plasticizers. Values as high as 10^{-6} S/cm at 80°C were found for two-phase mixtures with no added salt or plasticizers, *i.e.*, values comparable to or greater than those of recently developed dry single-ion conducting polymers. The increase in conductivity over that of the dry clay is due both to the increased interlayer spacing and to shielding of the cations from the negatively charged silicate sheets by the intercalated polymer. Other contributing factors may be decreased grain boundary resistance and space-charge effects, when small amounts of discrete polymer are present. Samples containing large excesses of polymer have extremely high resistances, however, especially at temperatures below the polymer melting point.

Conductivities for salt-containing mixtures are much higher than those with no added salt, and are comparable to those for simple binary salt-PEO systems without additives. These films have much better dimensional stability than those without laponite. The addition of a single-ion-conducting phase to the polymer electrolyte may allow less salt to be used, reducing the tendency for severe concentration polarization. Similarly, laponite may be used as a structural element in gels containing mixtures of salt, solvents or oligomers and polymers, to confer dimensional stability.

A characteristic break in the data is seen near the polymer melting point for samples containing excess PEO of molecular weight 100,000, and a changeover from Arrhenius to Vogel-Tamman-Fulgher (VTF) behavior occurs, indicating that segmental motion of the polymer dominates the conductivity behavior in the higher-temperature region. (This also serves to confirm that these systems are two-phase). No break is seen for materials containing the amorphous PEOs or for the nanocomposites which do not contain polymer as discrete phases. It is interesting to note that VTF behavior is also observed for many of these nanocomposites, particularly those with polymer contents near the maximum uptake limit. This suggests that a free-volume mechanism dominates the conductivity behavior. Rather than ion-hopping from site to site, polymer segmental motion between the silicate sheets propels the ions, as in most polymer electrolytes. Even so, conductivities in the nanocomposites are much lower than those of most PEO-salt complexes. In part, this is because nanocomposites are cationic conductors whereas both anions and cations conduct in polymer electrolytes, with anion mobility typically much greater. Intercalated polymers are also essentially restricted to two dimensions between the silicate sheets, reducing their free volume considerably compared to the free polymer. VTF fits to the data for true nanocomposites yield relatively high T^0 values, ranging from about 215-260 K, reflecting the reduced mobility (T^0 is typically about 30-50°C below the glass transition temperature). These results strongly suggest that conductivity can be further improved by increasing the inter-layer spacing, and/or incorporating oligomers or polar solvents. Cation motion would then be coupled to translational motion of the solvent between the layers, enhancing conductivity further. Unfortunately, our initial attempts at making such nanocomposites resulted in brittle films of little potential utility in practical devices. A possible solution to this problem is to form mixed nanocomposites containing both polymers and oligomers or solvents; these materials would have both good mechanical properties and high conductivities.

PUBLICATIONS

M.M. Doeff, A. Ferry, Y. Ma, L. Ding and L.C. De Jonghe, "Effect of Electrolyte Composition on the Performance of Sodium/Polymer Cells," *J. Electrochem. Soc.* **144**, L20 (1997).

A. Ferry, M.M. Doeff and L.C. De Jonghe, "Transport Property and Raman Spectroscopic Studies of the Polymer Electrolyte System $P(EO)_n$-NaTFSI," LBNL-40741, August 1997.

M.M. Doeff and L.C. De Jonghe, "Nanocomposite Polymer Electrolytes: Electrolyte Properties and Ion Transport," LBNL-40771A, October 1997.

M.M. Doeff and J.S. Reed, "Li-Ion Conductors Based on Laponite/Poly(Ethylene Oxide) Composites," LBNL-41050, November 1997. Invited paper A62, *11th International Conference on Solid State Ionics,* Honolulu, November, 1997, p. 79.

Polymer Electrolyte Synthesis for High-Power Batteries

John B. Kerr
62-203, Lawrence Berkeley National Laboratory, Berkeley, CA 94720
(510) 486-6279; fax: (510) 486-4995; e-mail: jbkerr@lbl.gov

Objectives

- Develop methods to prepare and characterize polymer electrolyte materials.
- Measure Li-ion transference numbers in polymer electrolytes.

Approach

- Optimize the preparation of polyvinylether and polyepoxide ether polymers containing from 2 to 8 ethylene oxide groups in the side chain.
- Use electrophoretic nuclear magnetic resonance (NMR) for transference measurements.
- Assess polymer purity and stability toward Li metal by half-cell cycling, impedance spectroscopy and post-test chemical analysis.

Accomplishment

- The thermal and transport property study on Parel (high-MW PPO)/$LiCF_3SO_3$ was completed.

Future Directions

- Complete transport measurements of amorphous PEO-LiTFSI, amorphous PEO-LiTf and PPO-LiTFSI.
- Perform photocalorimetry to determine the optimum conditions for photo-initiated polymerization of monomers or partially polymerized films.

Synthesis. Synthesis of vinyl-ether monomers used Williamson reaction conditions with diethyleneglycolvinyl ether and monomethyl ether of polyethylene glycol ethylchloride to give a variety of chain lengths from 2 to 7 ethylene oxide units. Several initiation systems were employed: BF_3-etherate at -78°C; Triflic acid at -78°C; $EtAlCl_2$ at 0°C; $Et_{1.5}AlCl_{1.5}$ at -45°C. The reaction could not be controlled with Triflic acid but BF_3 and $EtAlCl_2$ gave highly viscous polymers with MW $>10^5$. However, the material had high polydispersity indices (PDI > 3) with several MW fractions visible by gel permeation chromotrography (GPC). Fractionation gave little improvement and dialysis at elevated temperature resulted in depolymerization. The non-stoichiometric $Et_{1.5}AlCl_{1.5}$ gave polymers with increased MW from those reported previously in the literature, but the PDI ratio of 1.7-1.8 shows that a living polymer was not achieved.

Attempts were made to increase the MW by using more-controlled conditions, varying the initiator/monomer ratios and the use of chain-extension agents. Again the structure of these agents influences the MW of the polymer and excess cross-linker leads to the formation of intractable rubbers. The conditions for polymerization are still under development.

Synthesis of the capped a-PEO materials proved to be very irreproducible and it was found that the conditions used for the capping reactions lead to depolymerization. This indicates that the material is unstable to strongly acidic or highly oxidizing conditions. Considerable effort was made to correct this problem but it was avoided by elimination of the capping reaction.

Characterization of CB_X and CB_X/PPO Blended Electrolyte. All of the CB_x (x=2-7) materials were completely amorphous, as indicated by DSC measurements. The T_g is generally below -60°C before addition of Li salts, and increases with increasing salt concentration, particularly when the ratio of ether oxygen to Li ions (O/Li) is below 15:1. Although the tractable materials exhibited flow and did not form self-standing films, electrochemical measurements could be made by solution casting directly on to electrodes.

An alternative method to form self-standing films is to blend the CB_x materials with high-MW

PPO. This material was used to avoid the crystallinity problems that exist with PEO at low temperatures which has been thought to lead to *phase separation.* The PPO was Parel® Elastomer from Zeon Chemical (MW ~ $5x10^5$) which has a conductivity that is generally two orders lower than the CB_x polymers, indicating that the majority of the ion transport in the blends is *via* the CB_x material. However, severe phase separation also occurred which was dependent upon the concentration and identity of the Li salt. This result limits the use of polymer blends in binary salt electrolytes due to concentration polarization resulting from low Li^+ transference numbers.

Lithium Ion Transference Number (t_+^0) Measurements. The transference numbers were determined in collaboration with Peter Georen, Visiting Scholar from The Royal University of Technology (KTH), Chemistry and Chemical Engineering Department, Stockholm, Sweden. The thermal and transport property study on Parel (high-MW PPO)/$LiCF_3SO_3$ was completed. After an initial study of the thermal properties and conductivity, 85°C was chosen as the measurement temperature.

For the PPO/LiTf system, the preliminary results indicated that t_+^0 is positive only for very low salt concentrations and becomes increasingly negative as the salt concentration is increased, similar to the case with PEO/NaTf. Negative transference numbers have also been observed in liquid electrolytes, but the consequences are less severe, because of the generally higher salt diffusion coefficients and mobility of the solvent. Thus, it is critical to maximize t_+^0 in polymer electrolytes whenever possible.

The T_g of PPO/LiTf films were determined by DSC. No evidence of crystalline phases was observed by DSC nor did salt precipitation occur, a common problem in PPO-based electrolytes. The T_g values generally increased from -65°C for PPO_{400}LiTf to -8°C for PPO_3LiTf but two distinct thermal transitions were seen at intermediate salt concentrations (e.g., PPO_{20}LiTf), indicating a two-phase system. Visual inspection indicated that the films with this composition are clear, suggesting that micro-phase separation occurred.

The conductivity of PPO/LiTf samples was measured by AC impedance as a function of temperature and salt concentration. The data showed the VTF behavior typical of many polymer electrolytes and confirmed the DSC results, indicating that the system is substantially amorphous over this temperature and salt concentration range.

Salt diffusion coefficients were obtained from restricted-diffusion experiments on symmetrical cells containing the polymer electrolyte. These increased from 6.8×10^{-10} cm^2/sec for PPO_3LiTf to 1.6×10^{-8} cm^2/sec for PPO_{80}LiTf, although not monotonically.

Composite Polymer Electrolytes for Use in Lithium and Lithium-Ion Batteries

Saad A. Khan and Peter S. Fedkiw
Department of Chemical Engineering, North Carolina State University, P.O. Box 7905, Raleigh NC 27695-7905
(919) 515-4519; fax: (919) 515-3465; e-mail: khan@eos.ncsu.edu

Objectives

- Investigate the electrochemical and rheological characteristics of novel composite polymer electrolytes for Li and Li-ion batteries.
- Synthesize new fumed silicas with tailored surface chemistries for use in composite polymer electrolytes.

Approach

- Utilize electrochemical and rheological techniques to simultaneously study the effect of silica surface chemistry on the conductivity and mechanical properties of composite polymer electrolytes.

Accomplishments

- The conductivity of composite electrolytes was found to be independent of silica surface chemistry, and decreased only slightly with silica weight fraction. In all cases the conductivity exceeded 10^{-3} S/cm at room-temperature.

- By appropriately tailoring the silica surface chemistry, colloidal gels with elastic moduli exceeding 105 Pa was produced.

Future Directions

- Determine the transference number in candidate electrolyte systems using electrophoretic-NMR.
- Explore correlations between the silica surface chemistry and transference number, as well as the interfacial stability with Li.
- Develop a comprehensive understanding of the colloidal interaction forces responsible for gel formation (and hence mechanical stability) in these systems.

The objective of this research is to develop a new range of composite polymer electrolytes for use in rechargeable Li and Li-ion batteries. In particular, our goal is to develop highly conductive electrolytes which exhibit good mechanical properties (solid-like character), and at the same time show good compatibility with typical electrode materials. The unique feature of our approach is the use of surface-functionalized fumed silica fillers to control the mechanical properties of the electrolytes. A low molecular-weight liquid polyether is used as the matrix polymer, thereby ensuring high conductivities, and the fumed silica serves to provide mechanical support.

A key aspect of this approach is the ability to independently tailor the mechanical (rheological) and electrochemical behavior of the composites. To test the validity of this hypothesis, a range of surface-modified fumed silicas were synthesized, and the composite polymer electrolytes obtained from these novel fumed silicas were characterized. Electrolyte samples were prepared by dispersing the fumed silica in a matrix formed by PEGDME (MW ~ 250) and Li salt (typically lithium imide). The surface chemistries of the modified fumed silicas ranged from non-polar alkyl moieties (C_1 or C_8) to polar PEO oligomers (MW ~ 200).

Both the electrochemical and rheological behavior of the electrolytes were studied. It was found, rather surprisingly, that the conductivity of the electrolytes was essentially independent of the type of surface group present on the fumed silica. This is evident in Fig. 13 which shows the conductivity of composite electrolytes prepared using a variety of fumed silicas. Moreover, the conductivity is found to only decrease slightly on addition of fumed silica, even at high weight fraction of solids. In all cases, the room-temperature conductivity exceeds 10^{-3} S/cm.

In contrast to the conductivity, the rheological properties are strongly affected by both the fumed-silica surface chemistry and weight fraction. Dynamic rheological measurements reveal that fumed silicas with silanol and octyl coverage both flocculate into gels (networks). The resulting materials are mechanically stable, with the elastic modulus of the gel being strongly dependent upon weight fraction of solids. Gels with elastic moduli exceeding 105 Pa can be produced at high silica weight fractions (~ 20%). The PEO-modified fumed silica, on the other hand, gives rise to a low-viscosity suspension where the silica units exist as distinct non-interacting species.

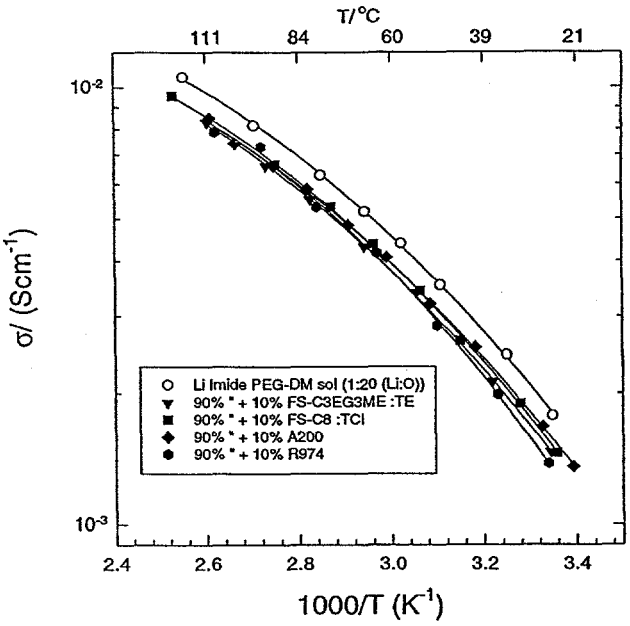

Figure 13. Effect of fumed-silica surface chemistry on conductivity. Data for conductivity as a function of temperature is shown for the base lithium imide.

These findings have powerful implications for future work on composite electrolytes in that the mechanical properties of the system can be tailored without affecting the conductivity. Further work is required to determine the effect of silica surface chemistry on the transport properties of Li^+ ions (*i.e.*, the Li^+ transference number), as well as the interfacial stability of composite electrolytes with

Li. In our earlier studies it was found that the addition of fumed silica contributed to a reduction and stabilization of the interfacial resistance. Work is ongoing in our laboratories to determine whether this effect is dependent on silica surface chemistry. Efforts to measure the transference number of composite electrolytes using electrophoretic-NMR are also under way.

Polymer Electrolyte for Ambient-Temperature Traction Batteries: Molecular-Level Modeling for Conductivity Optimization

Mark A. Ratner
Department of Chemistry, Northwestern University, Evanston IL 60208-3133
(847) 491-5371; fax: (847) 491-7713; e-mail: ratner@mercury.chem.nwu.edu

Objectives

- Analyze properties of polymer electrolytes by molecular dynamics and Monte Carlo simulations.
- Develop a microscopic understanding of the stability, structure and conduction properties of polymer electrolytes.
- Suggest modified materials with optimized conduction properties, based on mechanistic insight.

Approach

- Apply molecular dynamics and Monte Carlo simulation techniques to model and understand ion transport mechanisms.
- Use electronic structure methodologies to characterize ionic environments and energy barriers to diffusion.

Accomplishments

- Developed a simplified model for ionic motion in polyelectrolytes based on locally harmonic vibrational motions and on charge-trapping potentials. An analytic solution for the single-ion motion problem has been found.
- *Ab-initio* electronic structure calculations are showing excellent correlation with the few experimental data available on trapping barriers.

Future Directions

- Utilize *ab-initio* electronic structure calculations to compute effects of local site modification in determining barriers to ion transport in polyelectrolytes.
- Utilize a combination of Monte Carlo simulation and dynamic-bond percolation theory to investigate the effects of composite formation and grain-boundary conduction in hybrid polymer-based electrolyte materials.

There are two important mechanisms that impede ion transport in polymer electrolytes. The first of these is simple viscous drag: these electrolytes are dense materials, and ions cannot move unless relaxation properties of the polymer host permit such motion. We have therefore used a series of theoretical methods to investigate how the coupling between ion motion and polymer relaxation occurs, and to suggest different experimental modalities for increasing ion transport. The second effect of interion columbic coupling results in the formation of ion pairs and clusters, and can impede charge transport. Our recent work in this area has centered on polyelectrolytes: these are materials in which the transference number for Li is unity, so that no concentration polarization effects will be found. In the past, polyelectrolytes have been generally less conductive than polymer/salt complex materials. Optimization of polyelectrolytes involving reduced Lewis basicity has been carried out in Shriver's laboratory at Northwestern; our computational work is now centering on understanding what chemical substituents can be used to minimize site basicity, and therefore maximize ion mobility.

We have developed an analytical model that relates polymer chain stiffness, ion concentration, local ion site trapping (basicity) and temperature to ion diffusion coefficients. Based on this model, it is quite clear that local site basicity is a dominant process, one that is responsible for the generally reduced conduction in polyelectrolytes compared to polymer/salt complexes.

We have used *ab-initio* electronic structure calculations to investigate the local site basicity. The results indicate that substituents that lead to electronic delocalization away from the formal anionic site can substantially reduce basicities; calculated energy differences as large as 8 kilocal/mol have been observed. This work is carried out in collaboration with Dr. Larry Curtiss of the Chemical Technologies Division, Argonne National Laboratory.

While polyelectrolytes are a very attractive approach to optimize transference number and polarization effects, the overall mobility remains a critical factor. An important novel approach here has been to prepare nanocomposite structures that produce attractive physical rigidity properties while retaining local fluidity. We have begun modeling these composites, using our dynamic-bond percolation picture in concert with a particular picture for the local mobility at the interface. Preliminary results here are very promising, and suggest that such composite structures may indeed permit both rigidity and very fast ion motion in the appropriate conductive materials.

Corrosion of Current Collectors in Rechargeable Lithium Batteries

James W. Evans (Lawrence Berkeley National Laboratory)
585 Evans Hall, MC 1760, University of California, Berkeley CA 94720
(510) 642-3807; fax: (510) 642-9164; e-mail: evans@socrates.berkeley.edu

Objectives

- Examine corrosion of current collectors in Li-polymer and Li-ion batteries.
- Develop corrosion-resistant collectors and/or corrosion inhibition approaches.

Approach

- Use DC and AC electrochemical techniques to develop understanding of the corrosion behavior of current collectors and corrosivity of various electrolytes.
- Identify corrosion of current collectors in Li batteries under different charge conditions by SEM/energy dispersive X-ray (EDX) analyses.
- Develop corrosion-resistant alloys by ion-implantation or sputter deposition.

Accomplishments

- Serious corrosion of Al current collectors in Li-polymer batteries during overcharging was identified in three types of cells: (a) Li/V_6O_{13} (composite electrode), (b) Li/TiS_2 (composite electrode), and (c) Li/V_6O_{13} (thin-film electrode).

Future Directions

- Seek ways to modify the near surface of Al current collectors to enhance their resistance to corrosion.
- Continue evaluating the corrosion of battery container materials and the self discharge of Li-ion batteries.
- Develop understanding of corrosion mechanism/products by Auger electron spectroscopy (AES), electron spectroscopy for chemical analysis (ESCA), and/or surface-enhanced Raman spectroscopy (SERS).

Serious corrosion of Al current collectors in Li-polymer batteries during overcharging was identified in three types of cells: (a) Li/V_6O_{13} (composite electrode), (b) Li/TiS_2 (composite electrode), and (c) Li/V_6O_{13} (thin film electrode). To investigate the corrosion behavior and

mechanisms of the current collectors, electrochemical corrosion test techniques such as potentiodynamic scan and potentiostatic hold were used in conventional electrochemical corrosion cells (consisting of a working electrode, a counter electrode and a reference electrode). Only a few pits were observed on the Al working electrode, after repeated potentiodynamic anodic polarization and potentiostatic hold. Therefore, the design of corrosion tests which closely replicate battery operating conditions, and the interpretation of polarization curves as related to the corrosion behavior of current collectors in batteries remains a big challenge. To circumvent the discrepancy in corrosion test results between conventional corrosion cells and battery cells, efforts were made to unambiguously identify the corrosion phenomena by electrochemical polarization and by battery cycling techniques.

A possible corrosion mechanism was identified by comparing results from corrosion cells and battery cells, especially by investigating corrosion after galvanostatic holding of the Al working electrode of corrosion cells at large current densities. The variation of Al electrode potential during galvanostatic hold, in combination with SEM post-test examination, indicates the breakdown of aluminum oxide films on the Al surface. Therefore it is considered that a non-uniform electrical resistance/current distribution in the composite electrode, and thus on the Al current collector during battery overcharging, is the cause of current-collector corrosion. It is speculated that approaches leading to more-uniform current distribution (*e.g.*, coating an electrically conductive and corrosion-resistant layer on Al) will be effective in alleviating corrosion problems. If coatings break down during battery charging, then battery current collectors should be made from alternative corrosion-resistant alloys.

The corrosion behavior of aluminum, copper, nickel and stainless steels in liquid-electrolyte Li-ion batteries was also investigated. For electrolytes consisting of propylene carbonate (PC)/diethyl carbonate (DEC) solvents and different Li salts ($LiPF_6$, $LiClO_4$, $LiCF_3SO_3$, Li imide and Li methide), the corrosion of Cu, Ni and 302 stainless steel during potentiodynamic anodic polarization is serious, indicating possible corrosion problems for battery case materials. Serious corrosion of Al was observed in lithium triflate and lithium imide electrolytes. AES and ESCA were applied to identify corrosion products. Element depth profiles in current collectors and binding energy shifts suggest that fluoride from the lithium imide salt probably reacted with Al to form aluminum fluoride, and it was thus conjectured that a Li salt tending to release small anions may be more corrosive in non-aqueous solutions than in aqueous solutions. Charge/discharge cycling tests of commercial Sony Li-ion batteries were also conducted. Corrosion of the current collector under different charging conditions was identified. Post-test examination of current collectors showed corrosion of the Cu anode current collector after overdischarge, and the corrosion of Al cathode current collector in areas not covered with cathode materials, *e.g.*, in areas for connection to the electrical tab.

PRESENTATIONS

Y. Chen, L. Song, T.M. Devine and J.W. Evans, "Corrosion and Thermal Management in Advanced Batteries," *Automotive Technology Development Customer's Coordination Meeting*, Dearborn, MI, Oct. 29, 1997.

Y. Chen, L. Song, T.M. Devine and J.W. Evans, "Lithium Batteries: 1. Corrosion of Current Collectors, 2: Thermal Modeling in Support of Thermal Management," *Advanced Non-Aqueous Battery Technology: Research and Development Workshop*, Hunt Valley, MD, Oct. 15-17, 1997.

Development of Novel Chloroaluminate Electrolytes for High-Energy-Density Rechargeable Lithium Batteries

Kraig A. Wheeler
Department of Chemistry, Delaware State University, Dover DE 19901
(302) 739-4934; fax: (302) 739-3979; e-mail: kwheeler@dsc.edu

Objectives

- Develop electrochemically stable imidazolium chloroaluminate electrolytes.
- Characterize and investigate the electrochemical and physical properties of these electrolytic materials for lithium rechargeable battery (LRB) applications.

Approach

- Identify synthetically accessible imidazolium salts for fabrication of electrolytes.
- Evaluate electrochemical and spectroscopic properties of electrolytes.

Accomplishments

- Reproducibly synthesized 1-ethyl-3-methylimidazolium tetrachloroaluminate using nonaqueous, inert-atmosphere techniques.

Future Directions

- Develop and characterize organic-based electrolytes with improved electrochemical stability for LRBs.
- Determine the process of electrolytic degradation through coupled electrochemical-spectroscopic analysis.

This program focuses on the development of methods for the fabrication and characterization of novel electrolytes for high-energy-density battery applications. In this regard, chloroaluminate electrolytes comprise a class of organic-based materials that have shown promise in LRB applications.[1] This program studies the physical and electrochemical properties of 1-ethyl-3-methylimidazolium tetrachloroaluminate. Such studies provide information for the design and development of advanced organic-based electrolytes for LRBs.

To date, 1-ethyl-3-methylimidazolium tetrachloroaluminate (**4**) has been reproducibly synthesized using nonaqueous, inert-atmosphere techniques.[2] A systematic investigation of the preparation of chloroaluminate **4** resulted in the optimization of reaction conditions and the production of electrochemically pure material. The synthetic procedure involves the nucleophilic addition of 1-methylimidazole (**1**) and ethyl chloride (**2**) to give 1-ethyl-3-methylimidazolium chloride (**3**). Treatment of the organic salt **3** with ultra pure $AlCl_3$ resulted in 75-95 % yields of **4** as a colorless fluid. Increased sample purity of **4** could be obtained through repeated recrystallizations of the imidazolium chloride solid **3**.

It was shown that composition greatly affects the physical and electrochemical properties of chloroaluminate **4**. Three compositions of **3**:$AlCl_3$ were used: neutral (1:1, **3**:$AlCl_3$), basic (1:0.9, **3**:$AlCl_3$), and acidic (0.9:1, **3**:$AlCl_3$) mixtures.

The structure of chloroaluminate **4** was established by analysis of IR and ^1H NMR spectral data. Inspection of the IR spectrum (Fig. 14) of each mixture showed peaks consistent with C=C-H (3150 cm^{-1}) and C=N (1540 cm^{-1}) moieties. A comparative IR study of the basic, neutral and acid mixtures indicated a slight perturbation in the alkane region (3000-2900 cm^{-1}); even so, no significant structural changes in **4** could be assigned to this observation.

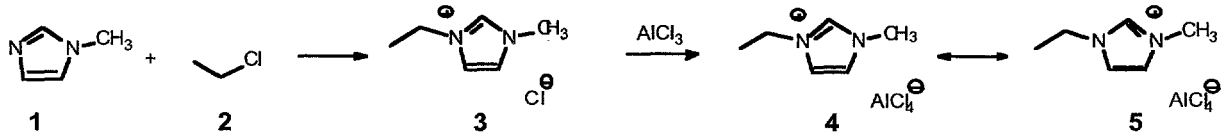

1 2 3 4 5

Analysis of the ^1H NMR spectrum confirmed the structure of **4** [(CDCl3) δ 10.77 (1 H, s), 7.51 (1 H, d, *J* = 7.5 Hz), 7.50 (1 H, d, *J* = 7.5 Hz), 7.48 (1 H, d, *J* = 7.5 Hz), 7.47 (1 H, d, *J* = 7.5 Hz), 4.39 (2 H, q, *J* = 7.1), 4.10 (3 H, s), 1.58 (3 H, t, J = 7.1). Resonances in the region 7.47 – 7.51 ppm correspond to an overlap of two doublet of doublets for the imidazole C(sp^3)-H groups. This pattern is consistent with the existence of resonance contributors (**4** and **5**) for the 1-ethyl-3-methylimidazolium cation. Additionally, both resonances at 4.39 and 4.10 ppm provide evidence for imidazolium cation formation as in **3** - **5**.

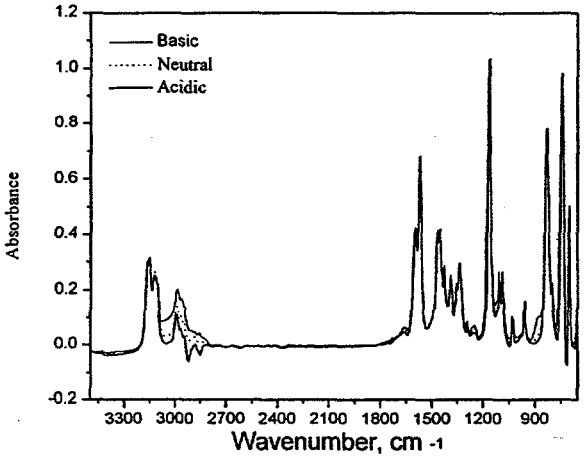

Figure 14. Infrared spectrum of neutral, basic, and acidic **4**.

The electrochemical properties of the chloroaluminate are illustrated in Fig. 15 as cyclic voltammograms. Inspection of the voltammetry reveals a dependence on the ratio of **3** and $AlCl_3$.[3] Neutral (1:1) chloroaluminate mixtures (Fig. 15a) possess remarkably wide electrochemical windows. Under these conditions, $AlCl_4^-$ is the predominant anion and the concentration of Cl^- and $Al_2Cl_7^-$ are both quite low. The electrochemical properties of the neutral electrolyte may be attributed to the stability of the $AlCl_4^-$ and imidazolium ions toward oxidative and reductive processes. Even though the shape of the voltammogram assigned to the basic mixture (Fig. 15b) resembles that of neutral **4**, the electrochemical window is significantly diminished. Under these conditions the lack of $Al_2Cl_7^-$ prevents imidazolium cation reduction as the cathodic background process. However, elevated concentrations of Cl^- prevent the oxidation of $AlCl_4^-$ as the anodic limit. As a result of free Cl^- in the basic mixture, chlorine production occurs at a lower potential reducing the electrochemical window. Inspection of Fig. 15c reveals the consequences of an acidic mixture of chloroaluminate **4**. Under these conditions $AlCl_4^-$ and $Al_2Cl_7^-$ are the predominant anions with suppressed Cl^- concentrations. While the anodic process is identical in the acid mixture to that observed in the neutral mixture, the cathodic limit is reached at potentials that are far less negative than to those necessary to reduce the imidazolium cation. Thus, the cathodic limit corresponds to the reduction of $Al_2Cl_7^-$ to deposit aluminum upon the electrode. For any given mixture, the decomposition potential for the predominant electroactive species determines the width of the electrochemical window.

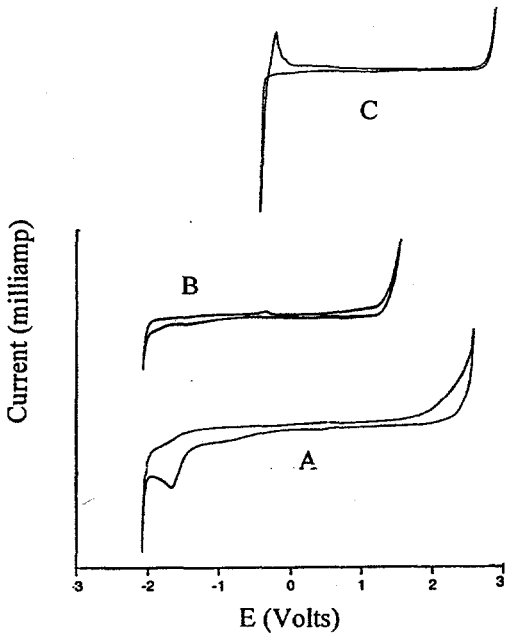

Figure 15. Cyclic voltammetry of **4** as neutral (a), basic (b), and acidic (c) mixtures.

The neutral mixture of chloroaluminate **4** was further characterized by *in situ* attenuated total reflectance (ATR) spectroscopy. Inspection of Fig. 16 provides evidence for a relationship between electrochemical reactions and infrared absorption by species existing in the neutral mixture. By applying an initial potential and stepping back to a reference potential (-1.8V and –0.4V) electroactive species could be analyzed as a function of time. The variation in the appearance of inflections at ≈ 3100 and 1600 cm^{-1} presumably corresponds to the degradation process of the 1-ethyl-3-methylimidazolium cation. The future goals of this project include understanding the

decomposition process of the electrolytic system toward the fabrication of electrolytes with advanced electrochemical properties. An understanding of these processes will greatly aid the design of tailor-made electrolytes for LRB applications.

REFERENCES

1. R.A. Carpio, L.A. King, F.C. Kibler, A.A. Fannin, *J. Electrochem. Soc.* **126**, 1650 (1979). J. Robinson, R.C. Bugle, H.L. Chem, D. Koran, R.A. Osteryoung, *J. Am. Chem. Soc.* **101**, 3776 (1979). N. Papageorgiou, Y. Athanassov, M. Armand, P. Bonhote, H. Pettersson, A. Azam, M. Gratzel, *J. Electrochem. Soc.* **143**, 3099 (1996). R.T. Carlin, C. Scordilis-Kelley, *J. Electrochem. Soc.* **141**, 873 (1994). C.L. Hussey, L.A. King, J.S. Wilkes, *J. Electroanal. Chem. Interfacial Electrochem.* **102**, 321 (1979).

2. J.S. Wilkes, J.A. Levisky, R. Wilson, C.L. Hussey, *Inorg. Chem.* **21**, 1263 (1982).

3. M. Lipstajn and R.A. Osteryoung, *J. Electrochem. Soc.* **130**, 1968 (1983).

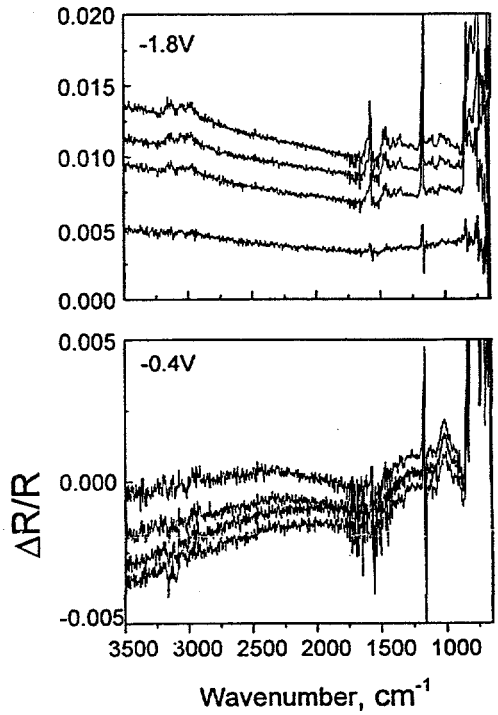

Figure 16. ATR spectrum of **4** showing IR absorbance as a function of potential and time.

CROSS-CUTTING RESEARCH

Cross-cutting research is carried out to address fundamental problems in electrochemistry, current-density distribution and phenomenological processes, solution of which will lead to improved electrode structures and performance in rechargeable batteries.

Analysis and Simulation of Electrochemical Systems

John Newman (Lawrence Berkeley National Laboratory)
201 Gilman Hall, MC 1462, University of California, Berkeley CA 94720
(510) 642-4063; fax: (510) 642-4778; e-mail: newman@newman.cchem.berkeley.edu

Objectives

- Improve the performance of electrochemical cells used in the interconversion of electrical energy and chemical energy by identifying the phenomena that control system performance.
- Identify important parameters which are crucial to the optimization of an advanced secondary battery.

Approach

- Utilize electrochemical engineering principles and advanced computer techniques to develop mathematical models.

Accomplishments

- Short-time experiments with intercalation electrodes have been fitted by a mathematical model using computer simulations and yielded reasonably constant fundamental diffusion coefficients of the Stephan-Maxwell transport equations.

Future Directions

- Secondary effects in the Li/polymer cell such as film formation and volume changes will be investigated.
- Continue Monte Carlo simulations to provide a theoretical basis for describing $Li_xMn_2O_4$ electrode behavior from first principles.
- System analysis is to be conducted using a combined battery and simple vehicle model.

This project carries out fundamental investigations of transport and interfacial phenomena important in electrochemical systems. Results of this work are used to analyze experimental data, to identify important system parameters, and to aid in the design and scale-up of electrochemical systems. The approach taken is to develop a detailed mathematical model of the electrochemical device using the principles of transport phenomena, reaction kinetics, and thermodynamics. The mathematical models are developed to be as general as possible without unnecessary mathematical or physical approximations. The resulting sets of coupled equations are then solved numerically, which permits the complex interactions between phenomena to be treated. Experimental work may then be used to confirm and refine the mathematical models and to determine the physical parameters necessary for a complete, quantitative understanding of the system.

Studies of intercalation electrodes have recently involved modeling of the short-time effects of potential variations. The system of interest has been a lithium manganese oxide porous electrode with a Li salt solution electrolyte; it is desired to discern the transport, thermodynamic and kinetic properties. Short-time cell behavior has the advantage of excluding side reaction and particle distribution effects. Short-time experiments have been fitted by a mathematical model using computer simulations. These simulations yielded reasonably constant fundamental diffusion coefficients of the Stephan-Maxwell transport equations. Cyclic voltammetry also enabled the determination of the open-circuit potential as a function of state of charge. The acquired transport and open-circuit information should prove useful in overall cell simulation.

Conceptual model development has been carried out for high-power capacitors. Work is to focus on the ruthenium oxide system involving several electrochemical processes. For an understanding of such a complex system, previously investigated systems which exhibit similar behavior have been studied. Also, related phenomena, such as pseudocapacitance, have been reviewed to gain preliminary mechanistic insight.

Further plans are proposed for the design of batteries for hybrid vehicles. System analysis will be conducted using a combined battery and simple vehicle model. This model helps to identify battery characteristics of importance in optimization. Guidelines are being developed for selection of battery systems. Initially, the selection criteria for an 'ideal' battery are to be established. Then, properties of real batteries may be considered to determine the relative importance to overall fuel efficiency for a particular vehicle design.

On the measurement of transport properties in polymer electrolytes, preliminary results have been obtained and plans made for the measurement of conductivity in the system of interest. A technique by Bellcore, Redbank, NJ, has been used for preparing the polymer electrolyte film, poly(vinylidene-fluoride/hexafluoropropylene), from liquid solution. Conductivity data were obtained by a.c. impedance spectroscopy. Refinement of the film preparation method should lead to satisfactory reproducibility of the measurements. The system has been initially modeled as binary (salt and polymer/solvent) requiring two additional experimental methods. In the long term, restricted diffusion and galvanostatic polarization have been planned to the obtain the diffusion coefficient(s) and the transference number of the system. Also, a concentration measurement would also be needed to

provide a thermodynamic reference for driving forces.

Computer programs which already describe the behavior of Li batteries are being modified and extended to simulate the performance of batteries under cycling and load profiles for hybrid electric vehicles (HEVs). Work is also being renewed on supercapacitors, both those based upon double-layer charging and those using Pt-Ru electrodes, which exhibit the characteristic known as pseudocapacitance. These devices will also be modeled to determine their performance under the load expected for a HEV driving profile.

Monte Carlo simulations have begun to provide a theoretical basis for describing $Li_xMn_2O_4$ electrode behavior from first principles.

PUBLICATIONS

M. Doyle and J. Newman, "Analysis of Capacity-Rate Behavior using Simplified Models for the Discharge Process of Lithium Batteries," *J. Appl. Electrochem.* **27**, 846-856 (1997).

S. Umino and J. Newman, "Temperature Dependence of the Diffusion Coefficient of Sulfuric Acid in Water," *J. Electrochem. Soc.* **144**, 1302-1307 (1997).

L. Rao and J. Newman, "Heat-Generation Rate and General Energy Balance for Insertion Battery Systems," *J. Electrochem. Soc.* **144**, 2697-2704 (1997).

R.M. Darling and J. Newman "On the Short-Time Behavior of Porous Intercalation Electrodes," *J. Electrochem. Soc.* **144**, 3057-3063 (1997).

J. Newman and W. Tiedemann, "Simulation of Recombinant Lead-Acid Batteries," *J. Electrochem. Soc.* **144**, 3081-3091 (1997).

B.K. Paxton and J. Newman, "Modeling of Nickel/Metal-Hydride Batteries," *J. Electrochem. Soc.* **144**, 3818-3831 (1997).

L.B. Fischel, D.N. Theodorou and J. Newman, "Segment Density of a Block Copolymer Chain Tethered at Both Ends," *J. Chem. Soc., Faraday Trans.* **93**, 4355-4370 (1997).

R. Darling and J. Newman, "Modeling a Porous Intercalation Electrode with Two Characteristic Particle Sizes," *J. Electrochem. Soc.* **144**, 4201-4208 (1997).

M.L. Perry, J. Newman and E.J. Cairns, "Mass Transport in Gas-Diffusion Electrodes: A Diagnostic Tool for Fuel-Cell Cathodes," *J. Electrochem. Soc.* **145**, 5-15 (1998).

Electrode Surface Layers

Frank R. McLarnon
90-1142 , Lawrence Berkeley National Laboratory, Berkeley CA 94720
(510) 486-4636; fax: (510) 486-4260; e-mail: frmclarnon@lbl.gov

Objectives

- Apply advanced *in situ* and *ex situ* characterization techniques to study the structure, composition and mode of formation of surface layers on electrodes used in rechargeable batteries.
- Identify film properties that improve the rechargeability, cycle-life performance, specific power, specific energy, stability and energy efficiency of electrochemical cells.

Approach

- Apply sensitive techniques such as ellipsometry, Raman spectroscopy, scanning probe microscopy, and impedance analysis to monitor the formation of surface layers on secondary battery electrodes.
- Incorporate foreign ions in porous nickel oxide electrodes to improve cycle performance in an alkaline electrolyte.
- Incorporate surface layers on Li electrodes to increase cycle life in nonaqueous electrolyte.

Accomplishments

- Tests of pasted NiOOH electrodes fabricated with surface-modified high-area microfiber Ni substrates demonstrated superior performance at high current densities.

- Initiated the first *in situ* ellipsometric characterization of carbon/nonaqueous-electrolyte interfaces.

Future Directions

- Complete investigation of the effect of Ni substrate modification on the electrochemical performance and durability of the NiOOH electrode.
- Employ *in situ* atomic-force microscopy in conjunction with electrochemical techniques to monitor changes in morphology and film thickness during the electrochemical reduction and oxidation of the NiOOH-$Ni(OH)_2$ electrode.
- Continue efforts to characterize the properties of pyrolytic carbon films fabricated from different materials and under various conditions using Raman spectroscopy, atomic-force microscopy and spectroscopic ellipsometry.

Advanced *in situ* and *ex situ* characterization techniques are being used to study the structure, composition and mode of formation of surface layers on electrodes used in rechargeable batteries. The primary objective of this research is to identify film properties that improve the rechargeability, cycle-life performance, specific power, specific energy, stability and energy efficiency of electrochemical cells. The present research seeks to characterize the transformation of surface phases that accompanies the charging and discharging of Ni electrodes in alkaline electrolytes and Li electrodes in nonaqueous electrolytes.

Nickel Electrodes. Electroprecipitated thin-film $Ni(OH)_2$ electrodes with Co and Li additives were characterized in detail by *in situ* Raman spectroscopy, and the effects of repeated charge-discharge cycling on the structure of discharged and charged films in dilute (1 M NaOH) and concentrated (7 M KOH) alkaline electrolytes were investigated. Electrochemical measurements showed that the presence of $Co(OH)_2$ in the film reduced the threshold potential for Ni^{2+} oxidation and inhibited the phase transitions which usually occur during prolonged cycling. In contrast, Li additions to the electrolyte improved the reversibility of the $Ni(OH)_2$-NiOOH redox reaction and reduced capacity fading during long-term cycling. Analysis of the Raman spectra confirmed that Co was incorporated into the $Ni(OH)_2$ lattice on Ni sites and a solid solution of $Co/Ni(OH)_2$ was formed. The structure of this electrochemically precipitated composite material was similar to that of chemically synthesized $Ni(OH)_2$. Lithium additions also led to significant structural modifications represented by two new vibrational bands at 615 and 660 cm^{-1} visible in Raman spectra of the reduced film. It was found that the properties of films in the presence of both Co and Li additives constituted a superposition of effects observed in single-additive composite $Ni(OH)_2$ electrodes.

We continued our research on the photo-electrochemical behavior of cathodically precipitated $Ni(OH)_2$ films on thin-film anatase TiO_2 substrates. Transparent $Ni(OH)_2$ films were electrochemically deposited onto TiO_2 layers which were formed on conductive glass. This composite optically transparent electrode exhibited strong reversible photochromic and photo-electrochromic properties when illuminated by a 75-W Xe lamp at open circuit and at anodic polarization in 1.0 M aqueous NaOH. The reversible transparent to black-gray coloration of the electrode upon UV-irradiation corresponded to the Ni^{2+}/Ni^{3+} redox reaction driven by the photogenerated charge carriers in the TiO_2 layer. Direct charge transfer between the photovoltaic TiO_2 film and the $Ni(OH)_2$ electrochromic film occurred at potentials 1.3 V more negative than the standard potential of $Ni(OH)_2/NiOOH$ couple. The rate and efficiency of electrode coloration depended on the intensity of the UV light, exposure time, and applied potential. Non-uniform illumination of the electrode produced a patterned optical state of the electrode which could be stored at positive polarization or erased at negative polarization. This new electrode is the subject of an invention disclosure, and represents an spin-off of our EV battery research to other applications.

We also sought to determine the effect of substrate modification on NiOOH electrode performance by the electrochemical deposition of fine Ni microparticles on the substrate prior to $Ni(OH)_2$ electroprecipitation. Modified-substrate NiOOH electrodes showed very good reversibility and substantially better long-term stability, compared to unmodified electrodes. Preliminary tests of pasted NiOOH electrodes fabricated with surface-modified high-area microfiber Ni substrates demonstrated superior performance at

high current densities. A series of chronoamperometric measurements on freshly precipitated $Ni(OH)_2$ electrodes showed a transient anodic current at potentials where Ni^{2+} is thermodynamically stable. This observation suggests that another anodic process proceeds at the interface between the Ni substrate and the $Ni(OH)_2$ film, *e.g.*, Ni passivation or nickel oxide sublayer formation. Modification of the substrate may have a significant effect on the properties and chemical composition of this interfacial layer, and thereby enhance the overall performance of the NiOOH electrode.

Lithium-Carbon Electrodes. Raman spectroscopy, coupled with high-resolution transmission electron microscopy (HRTEM) and X-ray diffraction analysis, were used to characterize the physical properties of carbonaceous materials obtained by heat treatment of petroleum coke at 1800, 2100 and 2350°C. The effects of heat treatment and an air-milling process (to obtain an average particle size of 10 μm) on the physical and microstructural properties of the carbon particles were examined. Raman intensities of the Δ and γ bands were used to estimate the crystallite size, and XRD was used to obtain the interplanar distance. We found that crystallographic parameters of this carbonaceous material are close those of graphite. The changes in the microstructure of petroleum coke were easily observed by Raman spectroscopy and complemented HRTEM observations. Distinct ordering of the layer planes accompanied heat treatment, and a perceptible difference in surface morphology was evident for petroleum coke heat treated at 2350°C and then air milled. Electrochemical results for Li intercalation/deintercalation into/from the petroleum cokes in 0.5 M $LiN(CF_3SO_2)_2$-EC-DMC electrolyte revealed that heat treatment at 2350°C improved the reversible Li storage capacity of the petroleum coke, and that air milling after heat treatment produced a petroleum coke with high reversible capacity, equivalent to $Li_{0.93}C_6$.

We initiated the first *in situ* ellipsometric characterization of carbon/nonaqueous-electrolyte interfaces. We first determined precise optical constants of highly ordered pyrolytic graphite (HOPG), glassy carbon and pyrolytic carbon prepared at different temperatures. Ellipsometry of a 1000°C-pyrolyzed photoresist film in 1:1 EC-DMC electrolyte with 1M $LiPF_6$ revealed that the as-formed interfacial layer was a relatively compact and ionically conductive SEI. The formation of this SEI was nearly complete after the first potential scan. Combined *in situ* spectroscopic ellipsometric data and *ex situ* XPS measurements suggested that the as-formed interfacial layer consisted of LiF and other ionically conductive compounds, and was well described by an effective-medium approximation model.

PUBLICATIONS AND PRESENTATIONS

L.M.M. de Souza, F.P. Kong, F.R. McLarnon and R.H. Muller, "Spectroscopic Ellipsometry Study of Nickel Oxidation in Alkaline Solution," *Electrochim. Acta* **42**, 1253-67 (1997).

R. Kostecki and F. McLarnon, "Electrochemical and *In Situ* Raman Spectroscopic Characterization of Nickel Hydroxide Electrodes I. Pure Nickel Hydroxide," *J. Electrochem. Soc.* **144**, 485-93 (1997).

R. Kostecki, T. Tran, X. Song, K. Kinoshita and F. McLarnon, "Raman Spectroscopy and Electron Microscopy of Heat-Treated Petroleum Cokes for Lithium-Intercalation Electrodes," *J. Electrochem. Soc.* **144**, 3111-17 (1997).

G. Zhuang, P.N. Ross Jr., F. Kong and F. McLarnon, "The Reaction of Clean Li Surfaces with Small Molecules in Ultrahigh Vacuum II. Water," *J. Electrochem. Soc.* **145**, 159-65 (1998).

F. Kong, R. Kostecki, F. McLarnon and R.H. Muller, "Spectroscopic Ellipsometry of Electrochemically Precipitated Nickel Hydroxide Films," presented by F. Kong at the *Second International Conference on Spectroscopic Ellipsometry*, Charleston, SC, May 1997.

F. Kong, R. Kostecki and F. McLarnon, "*In Situ* Ellipsometric Study of the Galvanostatic Deposition of Nickel Hydroxide Films," paper no. 48 presented by F. McLarnon at the *191st Meeting of the Electrochemical Society*, Montreal, Canada, May 1997.

F. Kong, G.R. Zhuang, K. Wang, P.N. Ross Jr. and F. McLarnon, "Application of Ellipsometry in Studying the Reactions of Li with Small Molecules in UHV," paper no. 355 presented by G.R. Zhuang at the *American Vacuum Society National Meeting*, San Jose, CA, October 1997.

Lithium Electrode Interfacial Studies

Philip N. Ross, Jr.
2-100, Lawrence Berkeley National Laboratory, Berkeley CA 94720
(510) 486-6226; fax: (510) 486-5530; e-mail: pnross@lbl.gov

Objectives

- Develop an understanding at the molecular level of the reactions that occur at the Li/electrolyte interface to form the SEI layer.
- Investigate the role of solute ions and solvent impurities (such as water) on the film-forming process.

Approach

- Apply a combination of ultrahigh vacuum (UHV) surface analytical methods and *in situ* ellipsometry.

Accomplishment

- Measurements indicate that Li reacts vigorously with water even at 160 K with LiOH as the majority reaction product in the presence of excess surface water.

Future Directions

- Study the interaction of Li with CO_2 using both the photoemission chamber and the ellipsometry chamber.
- Investigate other Li battery solvents that are esters chemically related to PC, including dimethylcarbonate (DMC) and diethylcarbonate (DEC).

Related prior work funded by Basic Energy Sciences established the proof-of-principal, that our proposed approach would elucidate the pathway of reactions between Li and battery solvents. In these proof-of-principal experiments, two prototypical Li battery solvents were studied, propylene carbonate (PC) and tetrahydrofuran (THF), the latter being a prototype of ethereal solvents. Polymerization of the THF (to poly-THF) occurs upon melting near 180 K, but is accompanied by chain-terminating reactions that form Li alkoxide(s) and hydrocarbon gas(es), such as ethylene and/or propylene. Between 180-320 K, there is progressively more conversion of poly-THF to alkoxide, such that at 320 K the surface film is predominantly Li alkoxide, only 1-2 ML thick. This layer effectively passivates the Li, because further exposure to THF at any temperature 120-320 K produces no further change in the layer thickness or composition. These surface reactions are consistent with the general observation that THF is a relatively unreactive solvent, and that Li cycling efficiency is highest in THF and related solvents, *e.g.*, 2-Me-THF. At or near its bulk melting temperature of 220 K, PC reacts with Li to form an alkyl carbonate. With increasing temperature, part of the alkyl carbonate decomposes to form an alkoxide, and at 270-320 K the film is a complex mixture of alkyl carbonate and alkoxide, with no evidence of formation of inorganic Li carbonate. As with THF, this film is only 1-2 ML thick and is essentially passive, being unreactive with subsequently deposited PC. Based on these results, PC is neither more nor less reactive with Li than THF.

We had also completed our first study of the reaction of Li with an important and ubiquitous impurity in Li battery electrolyte, water. Our results indicate that Li reacts vigorously with water even at 160 K with LiOH as the majority reaction product in the presence of excess surface water. The passivation layer is very thick, about 7 nm. However, the LiOH transforms into Li_2O through dehydration as excess water is removed from the surface by evaporation upon warming to room temperature. As a result, the Li_2O layer formed is porous in structure, but with very little metallic Li intermixed. Starting with thinner water overlayers, the resulting Li_2O layer is thinner and more compact, and contains a significant amount of metallic Li. At a fixed temperature, the absolute rate of reaction of water

with Li is much higher than the rate with either THF or PC. Unless the solvent is ultra-dry, the SEI layer on Li in a typical battery solvent is probably formed by the preferential reaction with water, i.e., Li_2O, which is not a good Li ion conductor and a poor SEI layer.

PUBLICATIONS

G. Zhuang, K. Wang and P. Ross, "XPS Characterization of the Reactions of Li with Tetrahydrofuran and Propylene Carbonate," *Surf. Sci.* **387**, 199 (1997).

G. Zhuang, P. Ross, F.-P. Kong and F. McLarnon, "The Reaction of Clean Li Surfaces with Small Molecules in Ultrahigh Vacuum: II. Water," *J. Electrochem. Soc.* **145**, 159 (1998).